https://doi.org/10.5194/egusphere-2026-3594
Preprint. Discussion started: 5 August 2026

Phytoplankton community, seasonality, and water chemistry modulate the lacustrine diurnal carbon engine and carbonate $\delta^{13}C$ values

Cedric J. Hagen[1,2], Elizabeth J. Trower[1], Andrea Halling[1], Sarah J. Hurley[3], Spruce W. Schoenemann[4], Miquela Ingalls[5], and Kathryn E. Snell[1]

[1]University of Colorado Boulder, Boulder, CO 80309, USA

[2]National Ecological Observatory Network, Battelle, Boulder, CO 80301, USA

[3]Lamont-Doherty Earth Observatory, Columbia University, Palisades, NY 10964, USA

[4]University of Montana Western, Dillion, MT 59725, USA

[5]The Pennsylvania State University, University Park, PA 16802, USA

Keywords: carbon isotopes, carbonate, paleoclimate, sedimentary facies, paleoenvironment

Corresponding Author: Cedric J. Hagen; Cedric.Hagen@Colorado.edu

Abstract

Stable isotopic measurements of carbon in carbonate rocks ($\delta^{13}C_{carb}$) have long been used to investigate paleoclimate and global carbon cycle dynamics. Recent work documented the diurnal carbon engine effect, which describes the impact of daily photosynthetic cyclicity on dissolved inorganic carbon (DIC) and, in turn, $\delta^{13}C_{carb}$ and $\delta^{13}C_{DIC}$ values, in low-latitude shallow marine environments. Because carbonate precipitation is temporally structured over the diurnal cycle, the resulting $\delta^{13}C_{carb}$ reflects a precipitation-weighted bias rather than a simple daily average. However, this system has not yet been explored in lakes. Here we present an adapted diurnal carbon engine model and constrain this effect for three end-member lake systems: Great Salt Lake (UT, USA), Green Lake (NY, USA), and Morrison Lake (MT, USA). We document how differing lake water chemistry and phytoplankton communities modulate local diurnal carbon engines. Because of geochemical and ecological differences, the impact of the diurnal carbon engine on $\delta^{13}C_{carb}$ values varies greatly by lake system. We estimated $\Delta^{13}C$ offsets, which represent the daily variability expected resulting from the diurnal engine and precipitation weighting, of ~0.36‰ in Great Salt Lake and ~0.24‰ in Green Lake. We also modeled how seasonality impacts the diurnal carbon engine in Great Salt Lake, which resulted in ~0.10‰ of $\delta^{13}C_{carb}$ variability. Modeled diurnal variability is consistent with observed dynamics in Green Lake. Predicted $\delta^{13}C_{carb}$ values are consistent with those measured from most carbonate sedimentary facies in each lake. Lacustrine $\delta^{13}C_{carb}$ shifts may reflect local environmental and ecological conditions, rather than changes in long-term lake $\delta^{13}C_{DIC}$ values or the global carbon cycle, complicating lacustrine $\delta^{13}C_{carb}$ record interpretations.

https://doi.org/10.5194/egusphere-2026-3594
Preprint. Discussion started: 5 August 2026

1 Introduction

Sediments and sedimentary rocks formed in lacustrine (lake) environments preserve valuable records of continental climate dynamics across Earth's history. One of the most important types of geochemical records is the measurement of stable carbon isotope ratios of carbonate sedimentary rocks (reported in delta notation as $\delta^{13}C_{carb} = \left[\frac{\left[\frac{^{13}C}{^{12}C}\right]_{carbonate}}{\left[\frac{^{13}C}{^{12}C}\right]_{standard}} - 1\right] \times 1000$) from both marine and lacustrine settings (e.g., Berner, 1990; Kump and Arthur, 1999; Zachos et al., 2001). While there are many ways that lacustrine $\delta^{13}C_{carb}$ records can be perturbed from equilibrium, excursions in $\delta^{13}C_{carb}$ are often linked to environmental or climatic events (e.g., Talbot, 1990; Valero-Garcés et al., 1997; Briner et al., 2006). These interpretations often assume that the dominant driver of $\delta^{13}C_{carb}$ change in lakes is global change in the $\delta^{13}C$ values of the marine–atmosphere system, which propagates into the dissolved inorganic carbon reservoir (DIC) of lakes. These same assumptions underlie efforts to relate fluctuations in $\delta^{13}C_{carb}$ records to variations in the global carbon cycle. Recent work has demonstrated that a number of other local-scale processes can impact carbon isotope values and our ability to interpret these measurements, including chemical alteration (e.g., Higgins et al., 2018; Swart and Oehlert, 2018), rock composition (i.e., sedimentary facies) variability (e.g., Ingalls et al., 2020; Geyman and Maloof, 2021), variation in biological mineralizers (e.g., Gischler et al., 2009), and the so-called "diurnal engine" (e.g., Geyman and Maloof, 2019; Trower et al., 2024).

The diurnal engine describes how daily fluctuations in the concentration of dissolved inorganic carbon (DIC) and pCO_2 result from the cyclic intensity of photosynthesis (due to the diel cycle). This in turn drives corresponding fluctuations in pH and carbonate mineral saturation states (see Zeebe and Wolf-Gladrow, 2001), and ultimately causes the carbon isotopic

https://doi.org/10.5194/egusphere-2026-3594
Preprint. Discussion started: 5 August 2026

composition of DIC ($\delta^{13}C_{DIC}$) to change. The carbon isotopic composition of DIC becomes relatively more enriched in ^{13}C during the day due to the preferential consumption of ^{12}C during photosynthesis and relatively more depleted in ^{13}C throughout the night due to the release of ^{12}C-enriched CO_2 through biological respiration (see **Figure 1**). Therefore, the diurnal engine suggests that bulk $\delta^{13}C_{carb}$ values can be offset from long-term, whole-lake average $\delta^{13}C_{DIC}$ values (often described as background $\delta^{13}C_{DIC}$ values) by a greater magnitude than would be predicted for carbonate minerals forming in equilibrium with long-term average DIC (often described as background DIC), depending on biases in the timing of carbonate formation during diel cycles; this effect complicates interpretations of $\delta^{13}C_{carb}$ records. These diurnal changes in water chemistry and their resulting consequences on $\delta^{13}C_{carb}$ values have been documented in several low-latitude shallow marine environments (Geyman and Maloof, 2019; Trower et al., 2024).

A key consequence of the diurnal engine is that changes in depositional environment, which can result in changes in primary productivity or isotopic fractionation and be recorded by sedimentary facies, could result in different offsets between $\delta^{13}C_{carb}$ and $\delta^{13}C_{DIC}$ values. Some secular fluctuations in $\delta^{13}C_{carb}$ records could therefore be entirely driven by the local diurnal carbon engine and not, in fact, reflect any external (or correlative) processes (see Background and **Figure 1**). The diurnal engine model implies that carbonate does not precipitate uniformly through time, but is biased toward periods of elevated saturation state, potentially amplifying isotopic offsets. Lacustrine $\delta^{13}C_{carb}$ records are often interpreted to be driven by global carbon cycle processes and thus reflect Cenozoic paleoclimate (e.g., Colman et al., 2007; Tanner, 2010; Rugenstein and Chamberlain, 2018; Lettéron et al., 2018; Benavente et al., 2021), and constraining how the diurnal engine effect modifies $\delta^{13}C_{carb}$ values is essential to being able to

https://doi.org/10.5194/egusphere-2026-3594
Preprint. Discussion started: 5 August 2026

accurately interpret these archives. For example, a relatively strong diurnal engine (>1‰ offset from predicted $\delta^{13}C_{carb}$ without a diurnal engine) could result in $\delta^{13}C_{carb}$ excursions that are erroneously interpreted as the result of global carbon cycle changes, but instead reflect a change in phytoplankton community, which in turn could be associated with a change in sedimentary facies. Said differently, an environmental change, recorded in sedimentary lithofacies, could modify the overall productivity of that environment, ultimately shifting κ_p (the photosynthetic forcing) and the local diurnal carbon engine. Likewise, an ecological shift in the dominant phytoplankton community could change background isotopic fractionation (ε_p, where $\varepsilon_p \approx \delta^{13}C_{CO_{2\,(aq)}} - \delta^{13}C_{biomass}$). Compared to shallow marine systems, lacustrine environments are often characterized by stronger spatial and temporal variability in productivity and carbonate saturation, suggesting that the magnitude and variability of the diurnal engine effect may be greater and more heterogeneous. Therefore, both environmental and ecological drivers could produce cryptic fluctuations in bulk $\delta^{13}C_{carb}$ values unrelated to sympathetic fluctuations in long-term average $\delta^{13}C_{DIC}$ values (as is often invoked when interpreting $\delta^{13}C_{carb}$ records). Note that environmental and ecological shifts are often related, further complicating the impact of carbon isotope records. Several recent studies in modern lacustrine settings have reported microbialite carbonate $\delta^{13}C_{carb}$ values that are up to 4‰ higher than predicted for carbonate minerals forming in isotopic equilibrium with average lake water DIC (Warden et al., 2016; Belan et al., 2019; White et al., 2021; Chen et al., 2022). These data provide compelling evidence that the diurnal engine effect is likely significant in lacustrine carbonate strata, suggesting that this mechanism may be responsible for and/or amplify or dampen some shifts in key lacustrine $\delta^{13}C_{carb}$ records (although these data could also be evidence for carbon limitation in microbial mats, changing ε_p).

https://doi.org/10.5194/egusphere-2026-3594
Preprint. Discussion started: 5 August 2026

At present, the parameters needed to model how diel cycling (and therefore the resulting photosynthetic forcing) controls the magnitude of the diurnal engine have only been somewhat constrained in marine environments (see Geyman and Maloof, 2019; Trower et al., 2024). Lacustrine photosynthetic communities are distinct from those found in shallow marine environments (e.g., Konopka and Brock, 1978; Hasle and Syversten, 1996), typically being dominated by freshwater algae or cyanobacteria rather than zooxanthellate reefs, marine algae, and marine cyanobacteria. Furthermore, many lakes have different physiochemical properties than the ocean, such as pH and buffering capacity, meaning lake carbonate chemistry can more easily shift between favoring dissolution and precipitation, ultimately impacting the timing of carbonate formation and the potential biases of $\delta^{13}C_{carb}$ values. Previously published constraints from marine systems are thus poor indicators for the lacustrine systems discussed herein. Furthermore, the enhanced seasonality and high spatial and temporal variation in primary productivity in carbonate-producing lakes relative to shallow tropical marine settings suggest that the magnitude and variability of the effect may be greater in lacustrine settings (e.g., Marshall and Peters, 1989; Catalan et al., 2002; Muchanga and Sichingabula, 2021). Here, we present a modified version of the Trower et al. (2024) diurnal engine model that facilitates new lacustrine applications, includes a new $\Delta^{13}C$ framework, and compares well with observational data. We employ this model to evaluate how productivity and alkalinity jointly control the magnitude diurnal isotopic offsets across a range of lacustrine conditions with a specific focus on seasonality and phytoplankton community. Together, these analyses provide a framework for understanding how diurnal carbon cycling influences lacustrine carbonate isotope records and how these effects may be distinguished from longer-term environmental change.

https://doi.org/10.5194/egusphere-2026-3594
Preprint. Discussion started: 5 August 2026

2 Background

2.1 Lacustrine stable carbon isotope dynamics

Traditionally, the fraction of organic carbon burial (f_{org}) (relative to the total carbon burial flux) has been used to explain carbon isotope fluctuations in marine carbonates as a function of environmental change (Kump and Arthur, 1999). For example, a global positive carbon isotope excursion could be explained by increased burial of organic carbon (i.e., higher f_{org}), which sequesters a greater proportion of ^{12}C in the lithospheric carbon reservoir. This, in turn, increases the $\delta^{13}C$ value of DIC ($\delta^{13}C_{DIC}$) in the ocean. While this framework for interpreting marine $\delta^{13}C$ excursions can be useful, work over the last couple of decades has demonstrated that $\delta^{13}C$ dynamics are often more complicated, with many other processes and carbon sources (e.g., methane hydrates or authigenic carbonate formation; Bjerrum and Canfield, 2011; Schrag et al., 2013) having the potential to drive large magnitude and global-scale perturbations in $\delta^{13}C$ records.

Lacustrine $\delta^{13}C$ records reflect many of the same processes and carbon sources as marine $\delta^{13}C$ records, allowing geochemists to apply the substantial body of research from marine settings to lacustrine settings. However, there are key differences, such as a substantially smaller DIC reservoir, distinct flora and fauna, and a greater importance of some carbon cycle processes (such as bedrock interaction and evaporation) (e.g., Leng and Marshall, 2004). Because of the large size of the oceanic reservoir, marine $\delta^{13}C$ variability is often assumed to reflect global processes (facilitating global chemostratigraphic correlation), with ocean mixing posing a minimum constraint on the temporal resolution (~1000 yr) of $\delta^{13}C$ records. In contrast, any given lake is significantly smaller than the ocean, and most carbonate-producing lakes are closed-basins, in which regional-scale evaporation and concomitant effects on organic matter

https://doi.org/10.5194/egusphere-2026-3594
Preprint. Discussion started: 5 August 2026

preservation can drive strong covariation between $\delta^{13}C_{carb}$ and $\delta^{18}O_{carb}$ isotopes, complicating global interpretations of $\delta^{13}C_{carb}$ records (e.g., Leng and Marshall, 2004). Processes on relatively short time scales (< 1000 yr) are rarely considered when assessing (marine or lacustrine) $\delta^{13}C$ records, much less daily variability (as discussed herein).

2.2 The diurnal carbon engine model for daily $\delta^{13}C_{carb}$ variability

The diurnal engine describes the daily transition from local carbon cycling dominated by aquatic photosynthetic organisms (e.g., green algae, cyanobacteria) during the day to carbon cycling dominated by heterotrophy at night (e.g., Geyman and Maloof, 2019; Trower et al., 2024). During the day, $\delta^{13}C_{DIC}$ values and the carbon isotope ratios of the carbonate minerals that precipitate from that DIC pool ($\delta^{13}C_{carb}$) increase, in addition to the rate of carbonate mineral formation, while $\delta^{13}C_{DIC}$ values, $\delta^{13}C_{carb}$ values, and the rate of carbonate mineral formation all decrease at night (**Figure 1**). These changes occur due to indirect effects of photosynthesis and aerobic respiration on the residual pool of DIC. The net effect of this process is that more carbonate precipitates when $\delta^{13}C_{DIC}$ values are elevated, meaning that bulk $\delta^{13}C_{carb}$ values of precipitated minerals will tend to more closely match daytime $\delta^{13}C_{DIC}$ values rather than daily averages (**Figure 1**). Although phototrophs and heterotrophs are abundant in most lakes and shallow marine environments, the magnitude of net photosynthetic forcing can vary significantly between and within ecosystems (e.g., Verduin, 1956; Carpenter et al., 1987; Howarth, 1988; Lewis Jr, 2011). This forcing affects the magnitude of change in $\delta^{13}C_{DIC}$ values, so when this forcing is small, $\delta^{13}C_{carb}$ values closely match the values predicted for carbonate minerals precipitating in equilibrium with average $\delta^{13}C_{DIC}$ values (see Geyman and Maloof, 2019; Trower et al., 2024). This key observation forms the basis of using $\delta^{13}C_{carb}$ values as proxies for

https://doi.org/10.5194/egusphere-2026-3594
Preprint. Discussion started: 5 August 2026

environmental or paleoclimatic change. In contrast, when the magnitude of photosynthetic forcing is large, like in modern coral reef environments (see Geyman and Maloof, 2019), the diurnal engine can lead to large differences (≥ 6‰) between actual and predicted $\delta^{13}C_{carb}$ values (e.g., Geyman and Maloof, 2019). These large differences complicate interpretations of this important geochemical proxy, meaning that an understanding of local diurnal carbon cycling and high-resolution, paired $\delta^{13}C_{carb}$–$\delta^{13}C_{org}$ measurements may be necessary to tease apart local and global $\delta^{13}C_{carb}$ signals. Furthermore, because carbonate precipitation rates vary through the diurnal cycle as a result of changes in carbonate mineral saturation state and temperature, resulting bulk carbonate isotopic compositions reflect a precipitation-weighted integration of $\delta^{13}C_{DIC}$ values rather than simply a daily average.

To date, the diurnal engine effect has only been quantified in equatorial, shallow marine carbonate islands (Geyman and Maloof, 2019; Trower et al., 2024), but this work has demonstrated that some positive $\delta^{13}C_{carb}$ excursions could be entirely driven by shifts in photosynthetic forcing rather than shifts in globally averaged marine $\delta^{13}C_{DIC}$ values as typically argued. Geyman and Maloof (2019) used a compilation of geochemical datasets from modern coral reef environments to posit a likely range of photosynthetic forcing in modern shallow marine environments. However, recent work conducted by Trower et al. (2024) found that a location on a modern carbonate platform (characterized by grainy sediment and sparse calcifying algae) resulted in photosynthetic forcing lower than almost all observed modern coral reefs. Therefore, local productivity appears to play a significant role in modulating the diurnal engine effect. Additionally, these findings demonstrate that the coral reef photosynthetic forcing parameters derived from the original diurnal engine study are not broadly representative of shallow marine environments with different photosynthetic communities, much less lacustrine

https://doi.org/10.5194/egusphere-2026-3594
Preprint. Discussion started: 5 August 2026

environments. Photosynthetic forcing could also vary significantly over small spatial scales (< 1 m) due to significant differences in productivity related to different photosynthetic communities (and environments, nutrients, etc.). In addition, because of the importance of local productivity in lakes, one cannot simply apply the marine diurnal engine values from previous work to lacustrine settings. In this contribution, we use a range of photosynthetic forcing values more representative of lakes to broadly explore the diurnal engine effect in lacustrine systems and suggest that future work seek to constrain this forcing in a variety of lacustrine systems.

2.3 Phytoplankton & carbon concentrating mechanisms

Primary producers are important to lake ecosystems, making them key to understanding biogeochemical and ecological change. Green algae and cyanobacteria are common primary producers in lakes with differing evolutionary backgrounds and ecological roles (e.g., Rockwell et al., 2014). Green algae are eukaryotes that rely on oxygenic photosynthesis, using chlorophylls a and c to capture light energy and convert carbon dioxide into organic compounds (e.g., Leliaert et al., 2012).

Cyanobacteria are divided into two groups (α-cyanobacteria and β-cyanobacteria) based on the type of carbon concentrating mechanism (CCM) they possess and the form of ribulose-1,5-bisphosphate carboxylase/oxygenase (RuBisCO) they encapsulate (1A and 1B RuBisCO, respectively). α-cyanobacteria and β-cyanobacteria exhibit adaptations that reflect their ecological niches and evolutionary histories (Badger et al., 2002). Broadly speaking, α-cyanobacteria are typically found in nutrient-poor, oligotrophic environments (e.g., marine) (e.g., Badger and Price, 2003). In contrast, β-cyanobacteria are broadly more commonly associated

https://doi.org/10.5194/egusphere-2026-3594
Preprint. Discussion started: 5 August 2026

with nutrient-rich, eutrophic waters (e.g., lakes) (e.g., Badger and Price, 2003). They also commonly form dense blooms (e.g., Huisman et al., 2018).

Both types of cyanobacteria and green algae are distinct in how they fix carbon. Specifically, cyanobacteria and green algae exhibit distinct CCMs that enhance their photosynthetic efficiency by increasing the local concentration of carbon dioxide around the enzyme responsible for fixing CO_2, RuBisCO. In cyanobacteria, the CCM is called a carboxysome, which is a proteinaceous microcompartment that encapsulates RuBisCO and carbonic anhydrase (Rae et al., 2013; Hill et al., 2020; Huffine et al., 2023). These cyanobacteria CCMs efficiently convert bicarbonate (HCO_3^-) into CO_2 directly at the site of RuBisCO, thereby minimizing photorespiration and enhancing carbon fixation efficiency even in low CO_2 conditions (Badger and Price, 2003). Additionally, cyanobacteria actively transport inorganic carbon species (CO_2 and HCO_3^-) into the cell using specialized transporters, further boosting intracellular CO_2 levels.

Green algae represent a broad designation with a variety of CCM strategies that are generally less understood when compared to cyanobacteria. Many green algae utilize pyrenoids, which are specialized structures within the chloroplasts that concentrate CO_2 around RuBisCO (Mackinder et al., 2016; Wang et al., 2023). These structures often work in conjunction with the active transport of HCO_3^- and CO_2 across cellular membranes, facilitated by carbonic anhydrases located in various cellular compartments, including the chloroplast stroma (Giordano et al., 2005). The exact mechanisms can vary significantly among different groups of green algae, reflecting their evolutionary diversity.

Distinct carbon concentrating mechanisms between α-cyanobacteria, β-cyanobacteria, and green algae result in different ranges of carbon isotopic fractionation (ε_P). α-cyanobacteria

https://doi.org/10.5194/egusphere-2026-3594
Preprint. Discussion started: 5 August 2026

containing alpha-carboxysomes and Form 1A RuBisCO are thought to produce a small range of ε_P values (~15.5–18.9‰; Popp et al., 1998). In contrast, β-cyanobacteria containing beta-carboxysomes and Form 1B RuBisCO inhabit a larger range of environments and produce a larger range of ε_P values (~7.7–22.7‰; Hurley et al., 2021). These diverse CCMs can cause variable magnitudes of fractionation under different environmental conditions, as they often involve multiple steps of carbon transport and conversion, which can preferentially select for ^{12}C or ^{13}C depending on the species and the specific pathway utilized (Giordano et al., 2005; Reinfelder, 2011).

3 Methods

3.1 Diurnal engine model framework

To evaluate the influence of diurnal variability on carbonate chemistry and isotopic composition, we employed a modified version of the diurnal carbon engine model presented by Trower et al. (2024) and based on the original description by Geyman and Maloof (2019). This model simulates coupled carbon cycling, gas exchange, and carbonate precipitation over a 24-hour period and is designed to capture transient, non-equilibrium behavior driven by diurnal biological forcing. The model presented here is not intended to exactly reproduce site-specific conditions, but rather to explore mechanistic relationships between environmental forcing and carbonate system dynamics. Specific model modifications from the Trower et al. (2024) code include: utilizing PHREEQC (Parkhurst and Appelo, 1999) for all water geochemistry calculations, as opposed to CO2SYS (Lewis and Wallace, 1998), because CO2SYS is explicitly designed for modern marine seawater and cannot be adapted for non-marine settings; translation

https://doi.org/10.5194/egusphere-2026-3594
Preprint. Discussion started: 5 August 2026

from MATLAB into R, a free and open-source language; and model parameter changes appropriate for lacustrine systems. For details about the full set of governing equations and model structure, please refer to Trower et al. (2024). This model is best described as a transient box model, designed to capture evolving, non-equilibrium conditions resulting from the dynamic, time-varying processes described herein. By design, the model is not forced to be mass- or isotope-conservative over each day, so it can be used to explore scenarios in which the system experiences hysteresis (conditions at the end of the day match those at the beginning of the day) and scenarios under which photosynthetic forcing might cause a net change in the aqueous chemistry of the system (conditions at the end of the day do not match those at the beginning of the day).

The model represents a well-mixed surface water layer subject to sinusoidal forcing of photosynthetic activity, parameterized by a productivity scaling term (κ_p). This forcing drives diurnal variability in dissolved inorganic carbon (DIC) through photosynthetic uptake during daylight hours and reduced uptake at night. Gas exchange with the atmosphere is included as a continuous process that moderates both DIC concentrations and isotopic composition. Carbonate precipitation is calculated as a function of carbonate mineral saturation state (Ω_{carb}), with precipitation occurring only when $\Omega > 1$. Precipitation rates increase nonlinearly with supersaturation following a kinetic formulation, capturing the strong dependence of carbonate formation on Ω_{carb} values and temperature. As a result, carbonate precipitation is not uniformly distributed through time, but instead preferentially occurs during periods of elevated saturation state. The isotopic composition of DIC ($\delta^{13}C_{DIC}$) is tracked dynamically, incorporating fractionation associated with gas exchange, biological uptake, and carbonate precipitation. The isotopic composition of precipitated carbonate is calculated as

https://doi.org/10.5194/egusphere-2026-3594
Preprint. Discussion started: 5 August 2026

$$\delta^{13}C_{carb} = \delta^{13}C_{DIC} + \varepsilon_{carb} \quad \text{Eq. 1}$$

where ε_{carb} represents the equilibrium fractionation between DIC and carbonate. To quantify the influence of diurnal variability of carbonate isotope signatures, we define the diurnal isotopic offset ($\Delta^{13}C$) as

$$\Delta^{13}C = \overline{\delta^{13}C_{carb,w}} - \left(\bar{\delta}^{13}C_{DIC} + \varepsilon_{carb}\right) \quad \text{Eq. 2}$$

where $\overline{\delta^{13}C_{carb,w}}$ is the precipitation-weighted mean isotopic composition of carbonate over the diurnal cycle and $\left(\bar{\delta}^{13}C_{DIC} + \varepsilon_{carb}\right)$ is the daily average instantaneous $\delta^{13}C_{carb}$ value. This formulation quantifies the isotopic bias introduced by preferential carbonate precipitation during daytime enrichment of DIC, relative to the expected $\delta^{13}C_{carb}$ predicted from the daily mean DIC composition. For comparison with observational data, modeled time series were aligned to observed peak saturation conditions to account for differences in temporal reference frames between modeled and measured datasets.

3.2 ε_p according to phytoplankton community and pCO_2

Carbon isotopic fractionation varies substantially among phytoplankton (e.g., Popp et al., 1998; Burkhardt et al., 1999; Marty and Planas, 2008; Brandenburg et al., 2022). Specifically, ε_p varies according to daylength, growth rate, pCO_2, cell geometry, and physiology (Popp et al., 1998; Burkhardt et al., 1999; Brandenburg et al., 2022). For example, ε_p can vary from 1.6–26‰ among diatoms, 17–25‰ among haptophytes, and 9.9–25‰ among freshwater green algae (Popp et al., 1998; Burkhardt et al., 1999; Marty and Planas, 2008).

https://doi.org/10.5194/egusphere-2026-3594
Preprint. Discussion started: 5 August 2026

Many different processes can impact photosynthetic carbon isotope fractionation, with growth rate and CO_2 availability being two of the more commonly discussed variables (e.g., Hollander and McKenzie, 1991; Botz et al., 1996; ŠantRůČková et al., 2000; Zhang et al., 2001; de Kluijver et al., 2014; Penger et al., 2014; Esposito et al., 2019; Hurley et al., 2019, 2021). For example, in Hurley et al. (2021) ε_P values (expressed as $\varepsilon_p = \delta^{13}C_{CO_{2\,(aq)}} - \delta^{13}C_{biomass}$) in a β-cyanobacterium varied largely as a function of CO_2 concentrations. Based on the data presented in Hurley et al. (2021), we used the following equation to estimate ε_p (in ‰) for β-cyanobacteria:

$$\varepsilon_p = \left(\frac{1}{[CO_2]} * -107.64\right) + 22.538 \quad \text{Eq. 3}$$

In the event that CO_2 concentration ($[CO_2]$) falls outside of the range of values reported in Hurley et al. (2021), we adopt the minimum and maximum ε_p values reported in Hurley et al. (2021) when $[CO_2]$ is below and above their reported range, respectively. In contrast, ε_p in α-cyanobacteria appears to be independent CO_2 availability (Popp et al., 1998). We therefore adopted a single mean value for ε_p (17.3‰) for α-cyanobacteria.

For this contribution, we arbitrarily adopt a general ε_p value of 14.5‰ for green algae (an average of multiple green algae ε_p values reported in the literature) but emphasize that the specific algae in question could lead to large differences in ε_p values and therefore modeled carbon isotope values (see **Figure S1** for a model sensitivity test varying ε_p from 9.9–25‰). Accurate modeling of the diurnal engine effect for a specific system should incorporate detailed knowledge of the photosynthetic community.

https://doi.org/10.5194/egusphere-2026-3594
Preprint. Discussion started: 5 August 2026

3.3 Modeling specific end-member environments

We created four different model configurations that incorporate geochemistry from four different environments and three different model phytoplankton taxa. These configurations include: water chemistry from the Turks and Caicos Islands with α-cyanobacteria (model scenario 1); water chemistry from the South Arm of Great Salt Lake with β-cyanobacteria (model scenario 2); water chemistry from Green Lake with green algae (model scenario 3); and estimated water chemistry for Morrison Lake with green algae (model scenario 4). These environments were chosen to represent different end-member environments where the diurnal engine likely operates including a marine carbonate platform (Caicos Platform, Turks and Caicos Islands), a high salinity lake (Great Salt Lake, Utah, USA), a freshwater lake (Green Lake, New York, USA), and a high elevation lake (Morrison Lake, Montana, USA). Furthermore, the phytoplankton communities present in these systems differ, with some being dominated by cyanobacteria (benthic mats and/or planktonic blooms) and others by green algae (benthic charophytes and planktonic green algae) (Culver and Brunskill, 1969; Koch and Madden, 2001; Larsen and Belovsky, 2013). Importantly, each of these systems produces carbonate (aragonite or calcite), allowing for the comparison of the diurnal engine across geochemical conditions and phytoplankton communities. We used mineral precipitation kinetics specific to the primary carbonate mineral forming in each environment.

3.3.1 Caicos Platform

The Caicos Platform (CP) is an archipelago southeast of the Bahamas (21.6940° N, 71.7979° W). Because the CP is a marine environment, the carbonate produced there is

https://doi.org/10.5194/egusphere-2026-3594
Preprint. Discussion started: 5 August 2026

aragonite, and the salinity of the water is ~35 g/kg. Note that most of the CP is a grainy sediment-dominated environment stabilized by algae (e.g., Wanless and Dravis, 1989; Trower et al., 2018) with modest productivity associated with green algae and patch reefs, while some protected intertidal lagoons host highly productive microbial mat communities with abundant and diverse α-cyanobacteria (e.g., Trembath-Reichert et al., 2016; Gomes et al., 2020; Lingappa et al., 2022; Stein et al., 2023; Trower et al., 2024). When modeling this environment, we used the carbonate and major ion chemistry configuration of Trower et al. (2024) (**Table 1**).

3.3.2 Great Salt Lake, Utah

Great Salt Lake (GSL) is a large hypersaline lake northwest of Salt Lake City, Utah (41.1158° N, 112.4768° W). Its salinity ranges from ~80–280 g/kg and it is a carbonate (aragonite) producing lake. Previous work has suggested that GSL microbial mat communities are dominated by cyanobacteria, the most abundant of which are halophilic coccoidal cyanobacteria *Euhalothece* sp. (Lindsay et al., 2017; Ingalls et al., 2020). Seasonal planktonic blooms of the green alga *Dunaliella viridis* are also an important mode of primary production in the lake (Baxter, 2018). Note that we are specifically modeling the South Arm of GSL, as the North Arm of GSL has even higher salinity and predominantly photoheterotrophic organisms and the halophilic green alga *Dunaliella salina* (Baxter, 2018). When modeling this environment, we used carbonate and major ion chemistry published by Ingalls et al. (2020) (**Table 1**) and represented primary production as dominated by β-cyanobacteria.

https://doi.org/10.5194/egusphere-2026-3594
Preprint. Discussion started: 5 August 2026

3.3.3 Green Lake, New York

Green Lake (GL) is a freshwater meromictic lake in Fayetteville, New York (43.0512° N, 75.9659° W) in which mixing does not occur, leading to the formation of deep, anoxic bottom waters (Brunskill and Ludlam, 1969). In addition to the photosynthetic microbial communities that contribute to growth of carbonate mounds on the steep basin margins, the calcifying algae, *Chara*, lines the shorelines (Thompson et al., 1990). Calcified thalli of these freshwater autotrophs comprise a significant fraction of the shallow, shoreline sediments (Leapaldt et al., 2024). The GL water column experiences an annual 'whiting' event (episodic water column precipitation of fine-grained calcium carbonate) that can last from one to several months (Stanton et al., 2023). The euhedral whiting crystals that form during these events are thought to be produced by a synergy in which the picocyanobacteria *Synechococcus* increases calcite saturation via photosynthesis and the diatoms (*Synechococcus*) and their associated EPS provide nucleation sites for carbonate growth (Stanton et al., 2023). In contrast to GSL (which precipitates aragonite), GL precipitates calcite (Brunskill, 1969). When modeling this environment, we used carbonate and major ion chemistry published by Leapaldt et al. (2024) (**Table 1**) collected in shallow (~1 m depth) water along shoreline adjacent to one of the GL thrombolite mounds.

3.3.4 Morrison Lake, Montana

Morrison Lake (ML) is a freshwater alpine lake in southwestern Montana (44.6019° N, 113.0367° W). ML is a high elevation lake (~2500 m.a.s.l.) that produces carbonate (calcite). ML is a closed basin lake fed by groundwater and underlain by carbonate bedrock (e.g., Thomas,

https://doi.org/10.5194/egusphere-2026-3594
Preprint. Discussion started: 5 August 2026

2019). These characteristics differentiate ML with GSL and GL, representing a different lake system endmember in terms of climate and seasonality. Furthermore, due to its latitude and elevation, ML is ice-covered for many months each year and likely is characterized by stronger seasonality than GSL and GL. There are no previously published lake chemistry data for ML. As such, we utilized pH data from ML and GL chemistry data as an approximation for ML (both GL and ML are freshwater carbonate-producing lakes) (**Table 1**) (**Data Set S1**). We did, however, manually set alkalinity higher at a mid-point value between the known values for GL and GSL (**Table 1**), as we found it unlikely that alkalinity is as low as GL at ML given the surrounding carbonate bedrock. ML, much like GL, experiences seasonal whitings that contribute carbonate to the sediment column (e.g., Stanton et al., 2023), but Leapaldt et al. (2024) demonstrated that carbonate precipitation occurs outside of whiting events in GL and we consider that this is likely the case for ML as well.

3.4 Model sensitivity and seasonality tests

In addition to the model scenarios described above, we also used model scenario 1 (representing the CP) to conduct model parameter sensitivity tests and model scenario 2 (representing the South Arm of GSL) to conduct phytoplankton community and seasonality tests. For the sensitivity tests, we varied the value of key model parameters over a wide range to assess its impact on key variables, such as [DIC] and $\delta^{13}C_{carb}$. The goal of these tests was to identify which model parameters have the largest impact on these key variables and are thus most important to constrain the diurnal carbon engine effect. For the phytoplankton community tests, we used identical GSL chemistry and diurnal carbon engine parameters, only changing the value of ε_p according to phytoplankton taxa (see Section 3.2) such that the impact of ε_p could be

https://doi.org/10.5194/egusphere-2026-3594
Preprint. Discussion started: 5 August 2026

assessed. For the seasonality tests, we modified temperature, wind speed, and the photosynthetic forcing function to simulate different seasons for model scenario 2. We used average daily temperatures and wind speeds reported for GSL in December, March, June, and September to represent winter, spring, summer, and fall, respectively. We modified the photosynthetic forcing function by increasing and decreasing its magnitude during the summer and winter, respectively (the function magnitude was not altered for spring or fall), and by adjusting its period according to the number of daylight hours at that time of year and latitude. We did not have separate geochemistry suites for each season and present this seasonality test as a broad preliminary result that should be followed up with additional data collection and model validation as part of future work.

4 Results

4.1 A flexible, free, and open-source diurnal carbon engine model

Using previously published and best estimates for lake geochemistry (see Methods), we used the diurnal engine model presented herein to model and estimate the magnitude of this effect in these four carbonate-producing settings (CP, GSL, GL, and ML). This diurnal engine model is very similar to the one presented by Trower et al. (2024) with only minor modifications made to handle lake geochemistry (see Methods). This new version is also written in R, making it free and open source to use. Note that this version of the diurnal engine model produced identical results for the marine CP (model scenario 1) as the model presented by Trower et al. (2024) (**Figure 2**).

https://doi.org/10.5194/egusphere-2026-3594
Preprint. Discussion started: 5 August 2026

4.2 Diurnal carbon engine model sensitivity tests

We conducted a series of sensitivity tests on model parameters and found that most parameters do not have a strong impact on the resulting magnitude of the diurnal carbon engine effect. However, we find that the photosynthetic forcing (referred to as the κ_p value following Trower et al. (2024) and Geyman and Maloof (2019)) has a strong control on the resulting carbonate chemistry and the magnitude of the isotopic response to the diurnal carbon engine (**Figure 3**). Solution chemistry also plays an important role, with lacustrine settings having displayed a marked difference from equatorial shallow marine settings (the only areas where this effect has been previously documented) (see **Figures 2 and 3**; model scenarios 1–2). Depending on the selected value for κ_p, $\delta^{13}C_{DIC}$ values fluctuated by $\geq 4‰$ in the Turks and Caicos Islands simulation (**Figure 3**). This sensitivity is consistent with observed diurnal variability in natural systems (see Section 4.6; Geyman and Maloof, 2019), where moderate productivity conditions reproduce observed carbonate system amplitudes.

4.3 The diurnal carbon engine varies between lacustrine systems

We also found that our diurnal carbon engine model predicts pronounced differences in the projected diurnal engine effect across the three lakes (model scenarios 2–4; **Figures 4 and 5**). Our model scenarios suggested that GSL is likely characterized by a smaller diurnal engine effect, in terms of the $\delta^{13}C_{carb}$ response, than GL and ML (**Figure 4**). Our results also suggested that seasonality plays a smaller role in shaping the effect in ML and GSL than in GL (**Figure 4**). However, it is important to note that ML is ice-covered in the winter, which likely alters the diurnal carbon engine; ice-coverage is not incorporated into these model scenarios, so our results

https://doi.org/10.5194/egusphere-2026-3594
Preprint. Discussion started: 5 August 2026

do not consider this effect. It would be valuable to collect field data during ice coverage to better understand how the carbonate system behaves when gas exchange and light penetration are very limited. We also found that the predicted carbonate saturation state (Ω_{carb}) was an order of magnitude higher in GL and ML than in GSL (~3.5–7 in GSL versus ~5–90 in GL and ML; **Figure 4**), although some of this difference results from mineralogy (aragonite in GSL; calcite in GL and ML) and ionic strength (ion activities in GSL are much more impacted by complexation due to high ionic strength than in the other lakes). In terms of the modeled carbon fluxes, the photosynthetic flux (F_{photo}) was identical across the model scenarios (as designed; **Figure 5**), but the carbonate precipitation flux (F_{carb}) and the gas exchange flux (F_{gas}) differed dramatically between the model scenarios. In terms of F_{carb}, GSL had relatively low values across the day (~0–0.6 µmol/kg/hr) while GL has values ranging up to ~8 µmol/kg/hr and ML had values exceeding 20 µmol/kg/hr (**Figure 5**). Importantly, F_{carb} was always positive throughout the entire model day in all three model scenarios, indicating that carbonate was never dissolving (**Figure 5**; which is expected, based on the Ω_{carb} values shown in **Figure 4**). Although carbonate precipitation occurs throughout the diurnal cycle in these simulations, rates vary strongly with saturation state, resulting in preferential precipitation during periods of elevation Ω. Lastly, F_{gas} also differed substantially between these three model scenarios, with values ranging between ~0 to –1.1 µmol/kg/hr in GSL, between -1 to 10 µmol/kg/hr in GL, and -1 to 1 µmol/kg/hr in ML (**Figure 5**). These model results predict that GSL is always a net CO_2 sink (lake pCO_2 < atmospheric pCO_2), while GL and ML are degassing at least some of the time (lake pCO_2 > atmospheric pCO_2). In summary, we found large, predicted differences between GSL, GL, and ML (model scenarios 2–4), which all in turn differ from the CP (model scenario 1).

https://doi.org/10.5194/egusphere-2026-3594
Preprint. Discussion started: 5 August 2026

We tested the impact of phytoplankton community, in terms of ε_p, on the diurnal carbon engine effect by systematically varying ε_p while holding all other model parameters constant (**Figure 6**; for these model simulations we used GSL chemistry values). We found that β-cyanobacteria produced the largest diurnal carbon engine effect, driving $\delta^{13}C_{DIC}$ 0.46‰ and $\delta^{13}C_{carb}$ 0.27‰ more positive than green algae, which resulted in the smallest positive shifts (**Figure 6**). α-cyanobacteria resulted in an intermediate magnitude diurnal carbon engine effect (in terms of $\delta^{13}C_{DIC}$ and $\delta^{13}C_{carb}$; **Figure 6**). These results demonstrate the importance of constraining the phytoplankton community (and its associated ε_p value) in order to best estimate the impact of the diurnal carbon engine on $\delta^{13}C_{DIC}$ and $\delta^{13}C_{carb}$ records. These differences highlight that the magnitude and temporal structure of the diurnal carbon engine are strongly system-dependent, reflecting differences in buffering capacity and carbonate precipitation dynamics.

4.4 The impact of seasonality on the diurnal carbon engine in Great Salt Lake

Many lacustrine systems, both modern and ancient, are not equatorial and are likely characterized by substantial seasonality. As depicted in **Figures 4 and 5**, seasonality does appear to impact the diurnal carbon engine. We conducted additional seasonality simulations for GSL (**Figure 7**), as we have more extensive geochemical and meteorological data for GSL in comparison with GL and ML. In these simulations, we varied temperature (T = 25°C, 18°C, -3°C, and 5°C; based on historical data for Salt Lake City, UT, from WeatherSpark), wind speed (u = 4.1 m/s, 3.8 m/s, 3.3 m/s, and 4.3 m/s; based on historical data for Salt Lake City, UT, from WeatherSpark), and productivity (κ_p = 190, 150, 110, and 150 µmol/kg; estimates based on Trower et al., 2024) according to season (summer, autumn, winter, and spring, respectively;

https://doi.org/10.5194/egusphere-2026-3594
Preprint. Discussion started: 5 August 2026

Figure 7). In terms of the modeled fluxes, summer had greatest magnitudes of F_{photo} values, followed by autumn and spring (identical, by design), and then winter (**Figure 7**); these differences are expected based on the chosen values for κ_p. Summer had the highest F_{carb} values, followed by autumn, and spring and winter (which were nearly identical; **Figure 7**). Lastly, for F_{gas}, winter had the largest magnitude flux, followed closely by spring, and then autumn and summer, which had significantly smaller fluxes (**Figure 7**). This finding suggests that, for our model conditions, GSL is always a CO_2 sink, even considering seasonality, but this net absorption of CO_2 is considerably stronger in the winter and spring months. In terms of the carbon isotopic response to a seasonally variable diurnal carbon engine in GSL, summer is always characterized by larger diurnal changes in both $\delta^{13}C_{DIC}$ and $\delta^{13}C_{carb}$ values, followed by autumn, and then very closely spring, and lastly winter (**Figure 7**). Note that the autumn and spring carbon isotopic responses are nearly indistinguishable, and that the net carbon isotopic response is only positive during the summer when the diurnal engine is strongest (**Figure 7**). Overall, our model simulations suggested that seasonality accounts for up to ~0.28‰ and ~0.10‰ of variability in $\delta^{13}C_{DIC}$ and $\delta^{13}C_{carb}$ values in GSL, respectively. Note that the initial $\delta^{13}C_{DIC}$ value does not exert a strong control on these results, with a sensitivity test indicating a ~0.05‰ and ~0.01‰ change in the seasonal variability of $\delta^{13}C_{DIC}$ and $\delta^{13}C_{carb}$ values, respectively, for each 1‰ shift in the initial $\delta^{13}C_{DIC}$ value (see **Figure S2**).

4.5 The diurnal carbon engine modulates $\delta^{13}C_{carb}$ records

Previous work has documented the potential importance of the diurnal carbon engine in shaping marine $\delta^{13}C_{carb}$ records (Geyman and Maloof, 2019; Trower et al., 2024). Our results have demonstrated that the same is true for lacustrine $\delta^{13}C_{carb}$ records (**Figures 2–8**). Assuming

https://doi.org/10.5194/egusphere-2026-3594
Preprint. Discussion started: 5 August 2026

constant major ion chemistry and summer temperature (25°C), we projected the carbon isotopic impact of the diurnal carbon engine across a range of productivity and alkalinity values in GSL (precipitating aragonite) and GL (precipitating calcite) (**Figure 8**). Aragonite (or calcite) precipitated with typical fractionation from DIC and the predicted aragonite (or calcite) precipitated with an active diurnal carbon engine differ. Using a modest productivity level (κ_p = 150 µmol/kg) and modern alkalinity for each lake (see red dots in the contour plots shown in **Figure 8**), we then estimated the predicted isotopic offset ($\Delta^{13}C$), defined as the difference between precipitation-weighted mean $\delta^{13}C_{carb}$ and the daily average instantaneous $\delta^{13}C_{carb}$ value (expected daily variability). This $\Delta^{13}C$ offset ranged from ~0–0.9‰ in GSL and ~0–3.9‰ in GL, with a much stronger dependence on productivity (κ_p) than alkalinity (**Figure 8**). For GSL, we calculated a precipitation-weighted mean $\delta^{13}C_{carb}$ value of ~2.81‰ and found an estimated $\Delta^{13}C$ offset of 0.03‰ (**Figure 8**). For GL, we calculated a precipitation-weighted mean $\delta^{13}C_{carb}$ value of ~ –5.64‰ and found an estimated $\Delta^{13}C$ offset of 0.27‰ (**Figure 8**). Note that we could not conduct these same tests for ML due to a lack of $\delta^{13}C_{DIC}$ data, but future field and lab work could allow for ML to be compared with GSL and GL.

4.6 Comparison to observed diurnal carbonate dynamics

To evaluate whether the model reproduces observed diurnal carbonate system behavior, we compared modeled diurnal variability in calcite saturation state (Ω) with digitized observations from Green Lake (Effler et al., 1981) (**Figure 9**). The model reproduces the timing and overall structure of the observed diurnal cycle, including nighttime minima and daytime maximum associated with photosynthetic CO_2 uptake. The magnitude of variability is sensitive to the productivity parameter (κ_p), with moderate values (κ_p = 100) producing amplitudes

https://doi.org/10.5194/egusphere-2026-3594
Preprint. Discussion started: 5 August 2026

comparable to observed summer conditions, while higher values produce larger amplitudes (**Figure 9**). This comparison demonstrates that the model captures first-order controls on biologically mediated carbonate chemistry in lacustrine systems while highlighting the importance of productivity in regulating diurnal variability.

5 Discussion

5.1 Timing of carbonate precipitation

While it is difficult to know when most carbonate is precipitating throughout the year for a given lake, it is clear that it is not only during seasonal whiting events (e.g., Stanton et al., 2023; Leapaldt et al., 2024). Our results indicate that the magnitude of isotopic offsets is controlled not simply by the extent of diurnal variability, but also by the timing of carbonate precipitation relative to that variability. Because precipitation rates are highest during periods of elevated saturation state, carbonate formation is inherently biased toward daytime conditions. Even if carbonate precipitation did only occur over a few weeks per year during these whiting events, diurnal variability would still matter during those events and ultimately influence $\delta^{13}C_{carb}$ values. If all carbonate precipitation occurred during a whiting (or 'bloom'), κ_p would likely be large at this time, meaning that the diurnal engine would result in an even stronger impact on $\delta^{13}C_{carb}$ values than it would if averaged out over the course of an entire year. Our standard model simulation assumes a temperature of 25°C meant to simulate summer conditions (unless otherwise stated, like for the seasonality tests). This is because in lacustrine settings, most carbon precipitates in the summer and precipitation rates are faster at warmer temperatures (e.g., Burton and Walter, 1987; Lopez et al., 2009; Romanek et al., 2011). Due to temperature–productivity

https://doi.org/10.5194/egusphere-2026-3594
Preprint. Discussion started: 5 August 2026

relationships (Konopka and Brock, 1978), κ_p would also likely be higher in summer. For these reasons, summer is when the diurnal engine is most likely to have an impact on sediment $\delta^{13}C_{carb}$ values.

5.2 Cryptic $\delta^{13}C_{carb}$ variability

Overall, we found large, predicted differences between CP, GSL, GL, and ML (model scenarios 1–4), which demonstrates that solution geochemistry, phytoplankton community, and seasonality all play important roles in shaping the diurnal carbon engine effect and thus $\delta^{13}C_{carb}$ records. A change in environmental conditions, as recorded in sedimentary lithofacies, could result in a change in the overall productivity of that environment, ultimately shifting κ_p and modifying the local diurnal carbon engine. Because κ_p reflects net photosynthetic forcing, it likely integrates multiple environmental controls such as light availability, nutrient supply, and phytoplankton community composition. Likewise, an ecological change resulting in a shift in the dominant phytoplankton community could change background isotopic fractionation (ε_p). Therefore, our results indicate that both environmental and ecological change (internal lacustrine system dynamics) could drive cryptic fluctuations in bulk $\delta^{13}C_{carb}$ values that are not related to sympathetic fluctuations in long-term average $\delta^{13}C_{DIC}$ values (external global dynamics; as is often invoked when interpreting $\delta^{13}C_{carb}$ records). As our modeling results demonstrated, the diurnal carbon engine can vary substantially between different lake environments due to lake geochemistry and phytoplankton community. As a result, instantaneous $\delta^{13}C_{carb}$ values vary throughout the course of each day (due to the diurnal carbon engine) and time of year (due to seasonality). This scale of temporal variability makes it difficult to tie sedimentary samples to specific environmental conditions. However, in some cases it may be possible to use proxies

https://doi.org/10.5194/egusphere-2026-3594
Preprint. Discussion started: 5 August 2026

(e.g., different isotopic signatures, lipid biomarkers) to better understand depositional environments and constrain diurnal engine impact at a given locality (e.g., Klatt et al., 2025; Olsen-Valdez et al., 2025). These findings underline the need to interpret lacustrine $\delta^{13}C_{carb}$ records in the context of changes in sedimentary facies, phytoplankton community, and seasonality, as κ_p (and therefore diurnal carbon engine strength) varies according to these environmental-ecological parameters and modulates $\delta^{13}C_{carb}$ records. Given the differences we predict in the diurnal carbon engine across these three lake systems, our findings also emphasize the need to ground truth the diurnal carbon engine in many different lake systems to establish suitable analogs for paleolacustrine $\delta^{13}C_{carb}$ record interpretation: κ_p is an empirical parameter that, to date, has only been estimated for zooxanthellate reefs and marine green algae in shallow tropical marine environments.

Comparing predicted $\delta^{13}C_{carb}$ values with those measured from GSL and GL, we can begin to better interpret these $\delta^{13}C_{carb}$ records. For GSL, our diurnal carbon engine model predicts typical $\delta^{13}C_{carb}$ values of ~2.8‰, based on modern lake chemistry and a modest κ_p estimate of 150 µmol/kg (**Figure 8**). Comparing this prediction with the sedimentary facies-specific $\delta^{13}C_{carb}$ values reported by Ingalls et al. (2020), we find that the prediction compares reasonably well with $\delta^{13}C_{carb}$ values measured from ooid-dominated facies (**Figure 8**). However, our predicted $\delta^{13}C_{carb}$ value does not compare well with those reported from mud-rich facies and carbonate coatings on anthropogenically-delivered silicate sand grains and microbialite samples (**Figure 8**). The ooid isotopic range reported by Ingalls et al. (2020) is a bit higher than our estimate (~4‰ vs ~2.8‰), and this is likely because ooids form slowly over long periods of time; in GSL, ooids have been accumulating over the past ~6000 years, with most of the carbonate precipitating prior to the Industrial Revolution (Paradis et al., 2024). For this reason,

https://doi.org/10.5194/egusphere-2026-3594
Preprint. Discussion started: 5 August 2026

the comparison of the $\delta^{13}C_{carb}$ values of these samples with modern $\delta^{13}C_{DIC}$ is complicated by the ^{13}C Suess Effect (Keeling, 1979), the phenomenon that the $\delta^{13}C$ value of atmospheric CO_2 (and DIC in surface fluids that equilibrate with the atmosphere) have increased due to anthropogenic carbon release. Atmospheric CO_2 $\delta^{13}C$ values have declined by about 2‰ since 1850 (Graven et al., 2020), implying that $\delta^{13}C_{DIC}$ values could have been 2‰ higher prior to 1850 when the carbonate in GSL ooids was precipitating. If we run the GSL model with an initial $\delta^{13}C_{DIC}$ value that is 2‰ higher, the model prediction (~4.78‰) compares better with the observed $\delta^{13}C_{carb}$ values of GSL ooids (~4‰). The microbialite sample $\delta^{13}C_{carb}$ values are even more positive than the ooid grainstones, and while the ^{13}C Suess Effect may also play a role in elevating these $\delta^{13}C_{carb}$ values, it cannot explain the larger magnitude of the positive offset of these samples. Instead, we interpret that it is more likely that microbial mats locally elevate productivity (and therefore κ_p), meaning that our relatively modest κ_p value of 150 µmol/kg is too low to accurately predict the $\delta^{13}C_{carb}$ values of these samples. Increasing κ_p would result in more comparable predicted $\delta^{13}C_{carb}$ values, and indeed, could allow us to place constraints on the productivity levels present when these microbialite samples precipitated.

In GL, measured $\delta^{13}C_{carb}$ values from a mud-rich charophyte setting and from a microbialite setting range from ~ –4 to –1‰ (Leapaldt et al., 2024). Both settings are relatively productive (dense charophyte beds and microbialite bioherms), so it is not surprising that the measured $\delta^{13}C_{carb}$ values are more positive than those predicted by our model (~ –5.64‰; this was also the case for the microbialite samples from GSL). To date, very few age constraints exist for the carbonate grains in GL, so we cannot directly constrain how much of this positive measured-predicted offset could be the result of the ^{13}C Suess Effect. We suspect that the ^{13}C Suess Effect plays an important role in shaping GL $\delta^{13}C_{carb}$ values, accounting for at least some

https://doi.org/10.5194/egusphere-2026-3594
Preprint. Discussion started: 5 August 2026

of the positive measured-predicted $\delta^{13}C_{carb}$ offset. As was the case for the measured GSL $\delta^{13}C_{carb}$ values, we interpret that it is likely that these charophyte and microbialite environments locally elevate productivity (and κ_p) and that our modest κ_p value of 150 µmol/kg is too low to accurately predict these GL $\delta^{13}C_{carb}$ values. Takahashi et al. (1968) present a dated carbonate core from GL, which suggests a reservoir age on the order of ~6000 yr. However, it is possible that this age reflects a deeper part of the lake which could have a different reservoir age (water depth at which the sediment core was collected is not reported), while the carbonate we are comparing our model predictions with formed in shallow depths (Leapaldt et al., 2024). Additional radiocarbon constraints from GL would be helpful in better understanding this system.

Because of the lack of $\delta^{13}C_{DIC}$ data from ML, we cannot confidently interpret the resulting $\delta^{13}C_{carb}$ values. Surface sediments from ML have been measured to have a $\delta^{13}C_{carb}$ value of –1.36‰ (S. Schoenemann, unpublished data), though we do not have the $\delta^{13}C_{DIC}$ and major ion chemistry measurements needed to accurately model the diurnal engine effect in ML. These additional geochemical data would greatly improve our understanding of ML. Comparison of modeled diurnal carbonate dynamics with observations from Green Lake further supports our interpretations (**Figure 9**). The model reproduces the timing and structure of observed diurnal variability, while the magnitude of variability is sensitive to productivity. This agreement suggests that the processes captured by this model are representative of real lacustrine systems, and that variability in productivity can explain differences in observed diurnal amplitude.

https://doi.org/10.5194/egusphere-2026-3594
Preprint. Discussion started: 5 August 2026

5.3 Model equilibrium

Depending on model scenario, $\delta^{13}C$ values do not always return to their starting values by the end of a diurnal cycle (e.g., Figure 4). This suggests that a baseline shift occurred during the day, and depending on model set up, could lead to a runaway effect if the model were run for many days. There are multiple explanations for this, depending on the specific model scenario.

First, the input model parameters may not have represented equilibrium (or realistic) conditions, forcing the model to end at different values than it started at. For example, the photosynthetic forcing function in diurnal engine models is not well constrained, as discussed earlier, and model scenarios with an especially strong photosynthetic forcing typically do not return to initial $\delta^{13}C$ values. Thus, a strong photosynthetic forcing could either be realistic and anomalous (e.g., a whiting event) for a given system, leading to a baseline geochemistry shift, or it could represent an unrealistic value for the given system, meaning that the predicted shift in geochemistry is also unrealistic (assuming the initial geochemistry is accurate). As another example, $\delta^{13}C_{DIC}$ values in lakes can vary seasonally, with higher values in the summer (commonly due to some combination of enhanced productivity and/or evaporation) than in other seasons; this pattern has been observed in Green Lake (Leapaldt et al., 2024) and a variety of other lakes (Mybro and Shapley, 2006; Bade et al., 2004; Hodell et al., 2003). [DIC] values and other aspects of lake water chemistry (i.e., major ion concentrations, which in turn reflect differences in salinity and alkalinity) can also vary seasonally; such variation has been documented in both Great Salt Lake and Green Lake (Ingalls et al., 2020; Leapaldt et al., 2024). Here, we chose the same initial conditions for our different tests of seasonality and phytoplankton community to most clearly show the impacts of these different variables on the magnitude of diurnal changes. Neglecting such seasonal changes (which are as yet not

https://doi.org/10.5194/egusphere-2026-3594
Preprint. Discussion started: 5 August 2026

adequately constrained in any of the example lakes to model appropriately) likely contributes to some of the predictions of baseline $\delta^{13}C_{DIC}$ values, which might be resolved which incorporation of better field data for a particular lake.

Second, it is important to note that there are biogeochemical processes not included in this model that can have an impact on $\delta^{13}C$ values, and that this model is, by design, not in perfect equilibrium (this is also true for all existing models of the diurnal engine; Trower et al., 2024; Geyman and Maloof, 2019). Evaporation, for example, could have a measurable impact on $\delta^{13}C$ values in these systems by further increasing $\delta^{13}C_{DIC}$ values during the daytime (e.g., Horton et al., 2016; Stiller et al., 1985), but it is not incorporated into this diurnal carbon cycling model. Similarly, mixing, including wind-driven mixing of waters between areas of differing productivity and/or water chemistry or seasonal mixing of stratified waters, would also influence the pattern of $\delta^{13}C$ values and is not included in the model scenarios presented here. Assuming processes like mixing and evaporation are sufficiently well constrained in a given lake system, their effects could easily be integrated with the diurnal carbon cycling model presented here in future implementations. While these caveats are important, we believe that the model results presented here still provide important and realistic constraints on lacustrine diurnal cycling, and specifically its impact on $\delta^{13}C_{carb}$ values, in most instances.

5.4 Implications for $\delta^{13}C_{carb}$ interpretations

Our findings predict $\delta^{13}C_{carb}$ offsets driven by the diurnal carbon engine, which differ according to productivity, lake geochemistry, and phytoplankton community (**Figure 8**). Our model results predict ~0.10‰ of variability in $\delta^{13}C_{carb}$ in GSL due to seasonality (**Figure 7**), and

https://doi.org/10.5194/egusphere-2026-3594
Preprint. Discussion started: 5 August 2026

we found $\Delta^{13}C$ offsets of 0.03‰ and 0.27‰ for GSL and GL, respectively (**Figure 8**). Therefore, many different variables (productivity, seasonality, water geochemistry, and phytoplankton community) conspire together to contribute variability to bulk $\delta^{13}C_{carb}$ signals, which essentially time-averages this variability. Figure 8 demonstrates that large diurnal variability does not necessarily produce isotopic bias; rather, bias emerges only where carbonate precipitation is sufficiently active and temporally structured. Thus, along with seasonal variability (**Figure 7**), both temporal forcing and system properties jointly control the magnitude of the diurnal carbon engine. This complicates point-to-point $\delta^{13}C_{carb}$ correlations (e.g., Hay et al., 2019; Hagen et al., 2024), as the absolute $\delta^{13}C_{carb}$ values may not be correlative. While normalized $\delta^{13}C_{carb}$ correlation may help address this problem, a new $\delta^{13}C_{carb}$ correlation scheme that can incorporate uncertainty in individual $\delta^{13}C_{carb}$ values would significantly improve correlation efforts with both marine and lacustrine $\delta^{13}C_{carb}$ records (see discussion in Hagen and Creveling (2024)). In some cases, it may be possible to tailor stratigraphic sampling resolution to account for suspected productivity, geochemistry, and phytoplankton in hopes of better capturing $\delta^{13}C_{carb}$ variability.

In terms of the predicted $\delta^{13}C_{carb}$ offsets, several studies have reported $\delta^{13}C_{carb}$ values in modern lacustrine carbonate microbialites that are up to 4‰ higher than expected for carbonate minerals forming in isotopic equilibrium with lake water DIC (Warden et al., 2016; White et al., 2021). This is consistent with the idea that the diurnal carbon engine is driving $\delta^{13}C_{carb}$ offsets in carbonate-producing lakes. Comparison of previously published $\delta^{13}C_{carb}$ data from GSL and GL reveal a similar observation: in both lakes, observed $\delta^{13}C_{carb}$ values of surface sediment are higher than predicted for carbonate minerals forming in isotopic equilibrium with modern lake water DIC (e.g., Ingalls et al., 2020; Leapaldt et al., 2024). While it is possible that this offset could be partially related to a time-averaging effect (i.e., surface sediments are old and

https://doi.org/10.5194/egusphere-2026-3594
Preprint. Discussion started: 5 August 2026

precipitated from lake water DIC that was substantially different from modern), we hypothesize that these data reveal the diurnal engine effect at play in both lakes. Additional data from ML would be very valuable, as it likely has a very small reservoir age correction (being shallow and well-mixed), eliminating the time-averaging issue.

6 Conclusions

In this contribution, we presented a diurnal carbon engine model framework to evaluate how diurnal variability and the timing of carbonate precipitation influence lacustrine $\delta^{13}C_{carb}$ values. In doing so, we demonstrated a large amount of variability in the diurnal carbon engine across lake systems and over the course of a year. Importantly, we show that isotopic offsets are governed not simply by the magnitude of diurnal variability, but by the timing of carbonate precipitation relative to that timing. Differences in lake geochemistry and dominant phytoplankton community appear to play a role in controlling the diurnal carbon engine and its impact on $\delta^{13}C_{DIC}$ and $\delta^{13}C_{carb}$ values. Both environmental and ecological changes can result in cryptic $\delta^{13}C_{carb}$ variability that is not directly linked to changes in long-term $\delta^{13}C_{DIC}$. We estimate that seasonality accounts for ~0.28‰ and ~0.10‰ of variability in $\delta^{13}C_{DIC}$ and $\delta^{13}C_{carb}$ in GSL, and that $\Delta^{13}C$ offsets are likely in excess of 0.03‰ and 0.27‰ in $\delta^{13}C_{carb}$ for GSL and GL, respectively. This variability may complicate $\delta^{13}C_{carb}$ correlations and the construction chronostratigraphic frameworks (see discussion in Hagen, 2024). Previously published $\delta^{13}C_{carb}$ data from carbonate-producing lakes are consistent with these findings, with comparable offsets between microbialites, surface sediment, and lake water DIC. These findings demonstrate that the interpretation of lacustrine $\delta^{13}C_{carb}$ records requires explicit consideration of both environmental variability and the timing of carbonate formation. While we provided a set of end-

https://doi.org/10.5194/egusphere-2026-3594
Preprint. Discussion started: 5 August 2026

member model scenarios, more lake environments should be incorporated into this modeling framework to provide more modern analogs for lacustrine $\delta^{13}C_{carb}$ records. Ground truthing our example lakes (GSL, GL, and ML) and additional lake environments will require extensive field campaigns collecting high temporal resolution water chemistry datasets over ≥ 24-hour periods. Furthermore, better constraints on κ_p are critical, as this parameter exerts primary control on diurnal carbon engine strength but has thus far only been estimated in marine systems. While a difficult parameter to constrain, it is necessary to estimate κ_p for each lake system with observational data. Ultimately, this framework provides a foundation for developing proxy system models capable of predicting $\delta^{13}C_{carb}$ records in paleolake environments and improving interpretation of these key paleoclimate archives.

Acknowledgements
Helpful conversations with C. Frantz, J. Olsen-Valdez, S. Dee, U. Lingappa, and J. Cameron significantly improved this work. We also acknowledge support and encouragement from the CU Chemical Sedimentology research group. We thank the anonymous reviewers and associate editor for their feedback that improved this contribution, as well as editor M.A. Xenopoulos for editorial handling.

Financial Support
We acknowledge support from NSF grant EAR-2234762 (to E.J.T.), University of Colorado Boulder Research and Innovation Office Seed grant (to E.J.T. and C.J.H.), and the NSF Graduate Research Fellowship Program (to A.H.).

Author contributions
C.J.H. and E.J.T. conceived the study, obtained funding, and developed the model; C.J.H. conducted model experiments with input from E.J.T, S.J.H., and A.H.; All authors contributed to discussions and manuscript review; C.J.H. wrote and edited the manuscript with input from E.J.T., S.J.H., A.H., S.J.H., S.W.S., M.I., and K.E.S. S.W.S. provided necessary data from Morrison Lake.

https://doi.org/10.5194/egusphere-2026-3594
Preprint. Discussion started: 5 August 2026

Supplementary Information

A Supplementary Information document includes two additional model output figures (Figures S1–S2), and a pH dataset from Morrison Lake, MT (Data Set S1).

Code and Data Availability

The model code used in this contribution is free and open-source, available in Zenodo: Hagen and Trower (2026; doi:10.5281/zenodo.20128480).

Competing Interests

The authors declare no conflicts of interest.

https://doi.org/10.5194/egusphere-2026-3594
Preprint. Discussion started: 5 August 2026

References

Bade, D. L., Carpenter, S. R., Cole, J. J., Hanson, P. C., Hesslein, R. H.: Controls of δ^{13}C-DIC in lakes: Geochemistry, lake metabolism, and morphometry, Limnology and Oceanography, 49, 1160–1172, 2004.

Badger, M. R., Hanson, D., Price, G. D.: Evolution and diversity of CO2 concentrating mechanisms in cyanobacteria, Functional Plant Biology 29, 161–173, 2002.

Badger, M. R., Price, G. D.: CO2 concentrating mechanisms in cyanobacteria: molecular components, their diversity and evolution, Journal of Experimental Botany 54, 609–622, 2003.

Baxter, B. K.: Great Salt Lake microbiology: a historical perspective, International Microbiology, 21, 79–95, 2018.

Belan, M. A., Brady, A. L., Kim, S. -T., Lim, D. S. S., Slater, G. F.: Spatial Distribution and Preservation of Carbon Isotope Biosignatures in Freshwater Microbialite Carbonate, ACS Earth and Space Chemistry, 3, 335–343, 2019.

Benavente, C. A., Mancuso, A. C., Bohacs, K. M.: Reconstructing Paleoenvironmental Conditions Through Integration of Paleogeography, Stratigraphy, Sedimentology, Mineralogy and Stable Isotope Data of Lacustrine Carbonates: An Example from Early Middle Triassic Strata of Southwest Gondwana, Cuyana Rift, Argentina, In: Limnogeology: Progress, Challenges and Opportunities : A Tribute to Elizabeth Gierlowski-Kordesch (eds. Rosen MR, Finkelstein DB, Park Boush L, Pla-Pueyo S). Springer International Publishing, Cham, pp. 471–509, 2021.

Berner, R. A.: Atmospheric Carbon Dioxide Levels Over Phanerozoic Time, Science, 249, 1382–1386, 1990.

Bjerrum, C. J., Canfield, D. E.: Towards a quantitative understanding of the late Neoproterozoic carbon cycle, Proceedings of the National Academy of Sciences, 108, 5542–5547, 2011.

Botz, R., Pokojski, H. -D., Schmitt, M., Thomm, M.: Carbon isotope fractionation during bacterial methanogenesis by CO2 reduction, Organic Geochemistry, 25, 255–262, 1996.

Brandenburg, K. M., Rost, B., Van de Waal, D. B., Hoins, M., Sluijs, A.: Physiological control on carbon isotope fractionation in marine phytoplankton, Biogeosciences, 19, 3305–3315, 2022.

Briner, J. P., Michelutti, N., Francis, D. R., Miller, G. H., Axford, Y., Wooller, M. J., Wolfe, A. P.: A multi-proxy lacustrine record of Holocene climate change on northeastern Baffin Island, Arctic Canada, Quaternary Research, 65, 431–442, 2006.

Brunskill, G. J.: Fayetteville Green Lake, New York. Ii. Precipitation and Sedimentation of Calcite in a Meromictic Lake with Laminated Sediments1, Limnology and Oceanography, 14, 830–847, 1969.

Brunskill, G. J., Ludlam, S. D.: Fayetteville Green Lake, New York. I. Physical and Chemical Limnology1, Limnology and Oceanography 14, 817–829, 1969.

Burkhardt, S., Riebesell, U., Zondervan, I.: Effects of growth rate, CO2 concentration, and cell size on the stable carbon isotope fractionation in marine phytoplankton, Geochimica et Cosmochimica Acta, 63, 3729–3741, 1999.

Burton, E. A., Walter, L. M.: Relative precipitation rates of aragonite and Mg calcite from seawater: Temperature or carbonate ion control?, Geology, 15, 111–114, 1987.

Carpenter, S. R., Kitchell, J. F., Hodgson, J. R., Cochran, P. A., Elser, J. J., Elser, M. M., Lodge, D. M., Kretchmer, D., He, X., Ende, C. N.: Regulation of Lake Primary Productivity by Food Web Structure, Ecology, 68, 1863–1876, 1987.

https://doi.org/10.5194/egusphere-2026-3594
Preprint. Discussion started: 5 August 2026

Catalan, J., Ventura, M., Brancelj, A., Granados, I., Thies, H., Nickus, U., Korhola, A., Lotter, A. F., Barbieri, A., Stuchlík, E., Lien, L., Bitušík, P., Buchaca, T., Camarero, L., Goudsmit, G. H., Kopáček, J., Lemcke, G., Livingstone, D. M., Müller, B., Rautio, M., Šiško, M., Sorvari, S., Šporka, F., Strunecký, O., Toro, M.: Seasonal ecosystem variability in remote mountain lakes: implications for detecting climatic signals in sediment records, Journal of Paleolimnology, 28, 25–46, 2002.

Caves Rugenstein, J. K., Chamberlain, C. P.: The evolution of hydroclimate in Asia over the Cenozoic: A stable-isotope perspective, Earth-Science Reviews 185, 1129–1156, 2018.

Chen, M., Conroy, J. L., Geyman, E. C., Sanford, R. A., Chee-Sanford, J. C., Connor, L. M.: Stable carbon isotope values of syndepositional carbonate spherules and micrite record spatial and temporal changes in photosynthesis intensity, Geobiology, 20, 667–689, 2022.

Colman, S. M., Yu, S. -Y., An, Z., Shen, J., Henderson, A. C. G.: Late Cenozoic climate changes in China's western interior: a review of research on Lake Qinghai and comparison with other records, Quaternary Science Reviews, 26, 2281–2300, 2007.

Culver, D. A., Brunskill, G. J.: FAYETTEVILLE GREEN LAKE, NEW YORK. V. STUDIES OF PRIMARY PRODUCTION AND ZOOPLANKTON IN A MEROMICTIC MARL LAKE1, Limnology and Oceanography, 14, 862–873, 1969.

Effler, S. W., Field, S. D., Wilcox, D. A.: The carbonate chemistry of Green Lake, Jamesville, New York, Journal of Freshwater Ecology, 1, 141–154, 1981.

Esposito, M., Achterberg, E. P., Bach, L. T., Connelly, D. P., Riebesell, U., Taucher, J.: Application of Stable Carbon Isotopes in a Subtropical North Atlantic MesocosmStudy: A New Approach to Assess CO2 Effects on the Marine Carbon Cycle, Frontiers in Marine Science, 6. 2019.

Geyman, E. C., Maloof, A. C.: A diurnal carbon engine explains 13C-enriched carbonates without increasing the global production of oxygen, Proceedings of the National Academy of Sciences, 116, 24433–24439, 2019.

Geyman, E. C., Maloof, A. C.: Facies control on carbonate δ13C on the Great Bahama Bank, Geology, 49, 1049–1054, 2021.

Giordano, M., Beardall, J., Raven, J. A.: CO2 CONCENTRATING MECHANISMS IN ALGAE: Mechanisms, Environmental Modulation, and Evolution, Annual Review of Plant Biology, 56, 99–131, 2005.

Gischler, E., Swart, P. K., Lomando, A. J.: Stable isotopes of carbon and oxygen in modern sediments of carbonate platforms, barrier reefs, atolls and ramps: Patterns and implications, Perspectives in Carbonate Geology: A Tribute to the Career of Robert Nathan Ginsburg: International Association of Sedimentologists Special Publication, 41, 61–74, 2009.

Gomes, M. L., Riedman, L. A., O'Reilly, S., Lingappa, U., Metcalfe, K., Fike, D. A., Grotzinger, J. P., Fischer, W. W., Knoll, A. H.: Taphonomy of Biosignatures in Microbial Mats on Little Ambergris Cay, Turks and Caicos Islands, Frontiers in Earth Science, 8, 2020.

Graven, H., Keeling, R. F., Rogelj, J.: Changes to Carbon Isotopes in Atmospheric CO2 Over the Industrial Era and Into the Future, Global Biogeochemical Cycles, 34, e2019GB006170, 2020.

Hagen, C.J.: Quantitative and nuanced approaches elucidate carbon isotope records, Geochemistry, Geophysics, Geosystems, 25, e2024GC011718, 2024.

https://doi.org/10.5194/egusphere-2026-3594
Preprint. Discussion started: 5 August 2026

Hagen, C. J., Creveling, J. R.: An algorithm-guided Ediacaran global composite δ13Ccarb–Bayesian age model, Palaeogeography, Palaeoclimatology, Palaeoecology, 650, 112321, 2024.

Hagen, C. J., Creveling, J. R., Huybers, P.: Align: A User-Friendly App for Numerical Stratigraphic Correlation, GSA Today, 34, 4–9, 2024.

Hagen, C. J., Trower, E. J.: Lakes C isotope model, Zenodo, https://doi.org/10.5281/zenodo.20128480, 2026.

Hasle, G. R., Syvertsen, E. E.: Marine diatoms, Identifying Marine Diatoms and Dinoflagellates, ed Tomas CR (Academic, San Diego), pp 5–385, 1996.

Hay, C. C., Creveling, J. R., Hagen, C. J., Maloof, A. C., Huybers, P.: A library of early Cambrian chemostratigraphic correlations from a reproducible algorithm, Geology, 47, 457–460, 2019.

Higgins, J. A., Blättler, C. L., Lundstrom, E. A., Santiago-Ramos, D. P., Akhtar, A. A., Crüger Ahm, A. -S., Bialik, O., Holmden, C., Bradbury, H., Murray, S. T., Swart, P. K.: Mineralogy, early marine diagenesis, and the chemistry of shallow-water carbonate sediments, Geochimica et Cosmochimica Acta, 220, 512–534, 2018.

Hill, N. C., Tay, J. W., Altus, S., Bortz, D. M., Cameron, J. C.: Life cycle of a cyanobacterial carboxysome, Science Advances, 6, eaba1269, 2020.

Hodell, D. A., Schelske, C. L., Fahnenstiel, G. L., Robbins, L. L.: Biologically induced calcite and its isotopic composition in Lake Ontario, Limnology and Oceanography, 43, 187–199, 2003.

Hollander, D. J., McKenzie, J. A.: CO2 control on carbon-isotope fractionation during aqueous photosynthesis: A paleo-pCO2 barometer, Geology, 19, 929–932, 1991.

Horton, T. W., Defliese, W. F., Tripati, A. K., Oze, C.: Evaporation induced ^{18}O and ^{13}C enrichment in lake systems: A global perspective on hydrologic balance effects, Quaternary Science Reviews, 131, 365–379, 2016.

Howarth, R. W.: Nutrient Limitation of Net Primary Production in Marine Ecosystems, Annual Review of Ecology and Systematics, 19, 89–110, 1988.

Huffine, C. A., Zhao, R., Tang, Y. J., Cameron, J. C.: Role of carboxysomes in cyanobacterial CO_2 assimilation: CO_2 concentrating mechanisms and metabolon implications, Environmental Microbiology, 25, 219–228, 2022.

Huisman, J., Codd, G. A., Paerl, H. W., Ibelings, B. W., Verspagen, J. M. H., Visser, P. M.: Cyanobacterial blooms, Nature Reviews Microbiology, 16, 471–483, 2018.

Hurley, S. J., Close, H. G., Elling, F. J., Jasper, C. E., Gospodinova, K., McNichol, A. P., Pearson, A.: CO2-dependent carbon isotope fractionation in Archaea, Part II: The marine water column, Geochimica et Cosmochimica Acta, 261, 383–395, 2019.

Hurley, S. J., Wing, B. A., Jasper, C. E., Hill, N. C., Cameron, J. C.: Carbon isotope evidence for the global physiology of Proterozoic cyanobacteria, Science Advances, 7, eabc8998, 2021.

Ingalls, M., Frantz, C. M., Snell, K. E., Trower, E. J.: Carbonate facies-specific stable isotope data record climate, hydrology, and microbial communities in Great Salt Lake, UT, Geobiology, 18, 566–593, 2020.

Keeling, C. D.: The Suess effect: 13Carbon-14Carbon interrelations, Environment International, 2, 229–300, 1979.

https://doi.org/10.5194/egusphere-2026-3594
Preprint. Discussion started: 5 August 2026

Klatt, A., De Jonge, C., Nelson, D. B., Reyes, M., Schubert, C. J., Dubois, N., Ladd, S. N.: Algal lipid distributions and hydrogen isotope ratios reflect phytoplankton community dynamics, Geochimica et Cosmochimica Acta, 394, 205–219, 2025.

Kluijver, A., Schoon, P. L., Downing, J. A., Schouten, S., Middelburg, J. J.: Stable carbon isotope biogeochemistry of lakes along a trophic gradient. Biogeosciences, 11, 6265–6276, 2014.

Koch, M. S., Madden, C. J.: Patterns of primary production and nutrient availability in a Bahamas lagoon with fringing mangroves, Marine Ecology Progress Series, 219, 109–119, 2001.

Konopka, A., Brock, T. D.: Effect of temperature on blue-green algae (cyanobacteria) in lake mendota, Appl Environ Microbiol, 36, 572–576, 1978.

Kump, L. R., Arthur, M. A.: Interpreting carbon-isotope excursions: carbonates and organic matter, Chemical Geology, 161, 181–198, 1999.

Larson, C. A., Belovsky, G. E.: Salinity and nutrients influence species richness and evenness of phytoplankton communities in microcosm experiments from Great Salt Lake, Utah, USA, Journal of Plankton Research, 35, 1154–1166, 2013.

Leapaldt, H. C., Frantz, C. M., Olsen-Valdez, J., Snell, K. E., Trower, E. J., Ingalls, M.: Primary to post-depositional microbial controls on the stable and clumped isotope record of shoreline sediments at Fayetteville Green Lake, Geobiology, 22, e12609, 2024.

Leliaert, F., Smith, D. R., Moreau, H., Herron, M. D., Verbruggen, H., Delwiche, C. F., De Clerck, O.: Phylogeny and Molecular Evolution of the Green Algae, Critical Reviews in Plant Sciences, 31, 1–46, 2012.

Leng, M. J., Marshall, J. D.: Palaeoclimate interpretation of stable isotope data from lake sediment archives, Quaternary Science Reviews, Isotopes in Quaternary Paleoenvironmental reconstruction, 23, 811–831, 2004.

Lettéron, A., Hamon, Y., Fournier, F., Séranne, M., Pellenard, P., Joseph, P.: Reconstruction of a saline, lacustrine carbonate system (Priabonian, St-Chaptes Basin, SE France): Depositional models, paleogeographic and paleoclimatic implications, Sedimentary Geology, 367, 20–47, 2018.

Lewis, E., Wallace, D.: Program developed for CO2 system calculations, Environmental System Science Data Infrastructure for a Virtual Ecosystem, 1998.

Lewis Jr, W. M.: Global primary production of lakes: 19th Baldi Memorial Lecture, Inland Waters, 1, 1–28, 2011.

Lindsay, M. R., Anderson, C., Fox, N., Scofield, G., Allen, J., Anderson, E., Bueter, L., Poudel, S., Sutherland, K., Munson-McGee, J. H., Van Nostrand, J. D., Zhou, J., Spear, J. R., Baxter, B. K., Lageson, D. R., Boyd, E. S.: Microbialite response to an anthropogenic salinity gradient in Great Salt Lake, Utah, Geobiology, 15, 131–145, 2017.

Lopez, O., Zuddas, P., Faivre, D.: The influence of temperature and seawater composition on calcite crystal growth mechanisms and kinetics: Implications for Mg incorporation in calcite lattice, Geochimica et Cosmochimica Acta, 73, 337–347, 2009.

Lingappa, U. F., Stein, N. T., Metcalfe, K. S., Present, T. M., Orphan, V. J., Grotzinger, J. P., Knoll, A. H., Trower, E. J., Gomes, M. L., Fischer, W. W.: Early impacts of climate change on a coastal marine microbial mat ecosystem, Science Advances, 8, eabm7826, 2022.

Mackinder, L. C. M., Meyer, M. T., Mettler-Altmann, T., Chen, V. K., Mitchell, M. C., Caspari, O., Freeman Rosenzweig, E. S., Pallesen, L., Reeves, G., Itakura, A., Roth, R., Sommer,

https://doi.org/10.5194/egusphere-2026-3594
Preprint. Discussion started: 5 August 2026

F., Geimer, S., Mühlhaus, T., Schroda, M., Goodenough, U., Stitt, M., Griffiths, H., Jonikas, M. C.: A repeat protein links Rubisco to form the eukaryotic carbon-concentrating organelle, Proceedings of the National Academy of Sciences, 113, 5958–5963, 2016.

Marshall, C. T., Peters, R. H.: General patterns in the seasonal development of chlorophyll a for temperate lakes, Limnology and Oceanography, 34, 856–867, 1989.

Marty, J., Planas, D.: Comparison of methods to determine algal δ13C in freshwater, Limnology and Oceanography: Methods, 6, 51–63, 2008.

Muchanga, M., Sichingabula, H. M.: Spatial and Seasonal Dynamics of Total Suspended Sediment, Total Dissolved Solids and Turbidity of a Lacustrine Reservoir in the Magoye Catchment, Southern Zambia, European Journal of Environment & Earth Sciences, 2, 43–48. 2021.

Myrbo, A., Shapley, M. D.: Seasonal water-column dynamics of dissolved inorganic carbon stable isotopic compositions ($\delta^{13}C_{DIC}$) in small hardwater lakes in Minnesota and Montana, Geochimica et Cosmochimica Acta, 70, 2699–2714, 2006.

Olsen-Valdez, J., Hagen, C. J., Widlansky, S. J., Trower, E. J., Snell, K. E., Clyde, W. C.: Photosynthetic carbon cycling signal preserved in carbonate δ13C values of ancient thrombolites, Geology, 53, 875–879, 2025.

Paradis, O., Corsetti, F., Bardsley, A., Hammond, D., Berelson, W., Xu, X., Walker, J., Celestian, A.: Radiocarbon Chronology/Growth Rates of Ooids from Great Salt Lake, Utah. *Geosites* **51**, 1–21, 2024.

Parkhurst, D. L., Appelo, C.: User's guide to PHREEQC (Version 2): A computer program for speciation, batch-reaction, one-dimensional transport, and inverse geochemical calculations, US Geological Survey, 1999.

Penger, J., Conrad, R., Blaser, M.: Stable carbon isotope fractionation of six strongly fractionating microorganisms is not affected by growth temperature under laboratory conditions, Geochimica et Cosmochimica Acta, 140, 95–105, 2014.

Popp, B. N., Laws, E. A., Bidigare, R. R., Dore, J. E., Hanson, K. L., Wakeham, S. G.: Effect of Phytoplankton Cell Geometry on Carbon Isotopic Fractionation, Geochimica et Cosmochimica Acta, 62, 69–77, 1998.

Rae, B. D., Long, B. M., Badger, M. R., Price, G. D.: Functions, Compositions, and Evolution of the Two Types of Carboxysomes: Polyhedral Microcompartments That Facilitate CO2 Fixation in Cyanobacteria and Some Proteobacteria, Microbiology and Molecular Biology Reviews, 77, 357–379. 2013.

Reinfelder, J. R.: Carbon Concentrating Mechanisms in Eukaryotic Marine Phytoplankton, Annual Review of Marine Science, 3, 291–315, 2011.

Rockwell, N. C., Lagarias, J. C., Bhattacharya, D.: Primary endosymbiosis and the evolution of light and oxygen sensing in photosynthetic eukaryotes, Frontiers in Ecology and Evolution, 2, 2014.

Romanek, C. S., Morse, J. W., Grossman, E. L.: Aragonite Kinetics in Dilute Solutions, Aquatic Geochemistry, 17, 339–356, 2011.

ŠantRůČková, H., Bird, M. I., Lloyd, J.: Microbial processes and carbon-isotope fractionation in tropical and temperate grassland soils, Functional Ecology, 14, 108–114, 2000.

Schrag, D. P., Higgins, J. A., Macdonald, F. A., Johnston, D. T.: Authigenic Carbonate and the History of the Global Carbon Cycle, Science, 339, 540–543, 2013.

https://doi.org/10.5194/egusphere-2026-3594
Preprint. Discussion started: 5 August 2026

Stanton, C., Barnes, B. D., Kump, L. R., Cosmidis, J.: A re-examination of the mechanism of whiting events: A new role for diatoms in Fayetteville Green Lake (New York, USA), Geobiology, 21, 210–228, 2023.

Stein, N. T., Grotzinger, J. P., Quinn, D. P., Lingappa, U. F., Present, T. M., Trower, E. J., Gomes, M. L., Orzechowski, E., Cantine, M., Metcalfe, K. S., Fischer, W. W., Ehlmann, B. L., Strauss, J. V., Knoll, A. H.: Geomorphic and environmental controls on microbial mat fabrics on Little Ambergris Cay, Turks and Caicos Islands, Sedimentology, 70, 1915–1944, 2023.

Stiller, M., Rounick, J. S., Shasha, S.: Extreme carbon-isotope enrichments in evaporationg brines, Nature, 316, 434–435, 1985.

Swart, P. K., Oehlert, A. M.: Revised interpretations of stable C and O patterns in carbonate rocks resulting from meteoric diagenesis, Sedimentary Geology, 364, 14–23, 2018.

Takahashi, T., Broecker, W., Li, Y. H., Thurber, D.: CHEMICAL AND ISOTOPIC BALANCES FOR A MEROMICTIC LAKE, Limnology and Oceanography, 211–401, 1968.

Talbot, M. R.: A review of the palaeohydrological interpretation of carbon and oxygen isotopic ratios in primary lacustrine carbonates, Chemical Geology: Isotope Geoscience section, 80, 261–279, 1990.

Tanner, L. H.: Chapter 4 Continental Carbonates as Indicators of Paleoclimate, In: Developments in Sedimentology, Carbonates in Continental Settings: Geochemistry, Diagenesis and Applications (eds. Alonso-Zarza AM, Tanner LH). Elsevier, pp. 179–214, 2010.

Thomas, J. E.: Holocene Paleoclimatic Reconstructions of the Northern Rocky Mountains as Determined From Stable Isotope Analysis of Carbonate Minerals and Organic Matter in Sediments From Morrison Lake, MT (M.Sc.), 2019.

Trembath-Reichert, E., Ward, L. M., Slotznick, S. P., Bachtel, S. L., Kerans, C., Grotzinger, J. P., Fischer, W. W.: Gene Sequencing-Based Analysis of Microbial-Mat Morphotypes, Caicos Platform, British West Indies. *Journal of Sedimentary Research* **86**, 629–636, 2016.

Trower, E. J.: Caicos Platform C isotope model, Zenodo, https://doi.org/10.5281/zenodo.10022912, 2024.

Trower, E. J., Cantine, M. D., Gomes, M. L., Grotzinger, J. P., Knoll, A. H., Lamb, M. P., Lingappa, U., O'Reilly, S. S., Present, T. M., Stein, N., Strauss, J. V., Fischer, W. W.: Active Ooid Growth Driven By Sediment Transport in a High-Energy Shoal, Little Ambergris Cay, Turks and Caicos Islands, Journal of Sedimentary Research, 88, 1132–1151, 2018.

Trower, E. J., Hibner, B. M., Lincoln, T. A., Dodd, J. E., Hagen, C. J., Cantine, M. D., Gomes, M. L.: Revisiting Elevated $\delta^{13}C$ Values of Sediment on Modern Carbonate Platforms, Geophysical Research Letters, 51, e2023GL107703, 2024.

Valero-Garcés, B. L., Laird, K. R., Fritz, S. C., Kelts, K., Ito, E., Grimm, E. C.: Holocene Climate in the Northern Great Plains Inferred from Sediment Stratigraphy, Stable Isotopes, Carbonate Geochemistry, Diatoms, and Pollen at Moon Lake, North Dakota, Quaternary Research, 48, 359–369, 1997.

Verduin, J.: Primary Production in Lakes, Limnology and Oceanography, 1, 85–91, 1956.

Wang, R. Z., Nichols, R. J., Liu, A. K., Flamholz, A. I., Artier, J., Banda, D. M., Savage, D. F., Eiler, J. M., Shih, P. M., Fischer, W. W.: Carbon isotope fractionation by an ancestral

https://doi.org/10.5194/egusphere-2026-3594
Preprint. Discussion started: 5 August 2026

rubisco suggests that biological proxies for CO2 through geologic time should be reevaluated, Proceedings of the National Academy of Sciences, 120, e2300466120, 2023.

Wanless, H. R., Dravis, J. J.: Carbonate Environments and Sequences of Caicos Platform: Caicos, British West Indies to Miami, Florida, July 20-26, 1989, Wiley Online Library, 1989.

Warden, J. G., Casaburi, G., Omelon, C. R., Bennett, P. C., Breecker, D. O., Foster, J. S.: Characterization of Microbial Mat Microbiomes in the Modern Thrombolite Ecosystem of Lake Clifton, Western Australia Using Shotgun Metagenomics, Frontiers in Microbiology, 7, 2016.

White, R. A., Visscher, P. T., Burns, B. P.: Between a Rock and a Soft Place: The Role of Viruses in Lithification of Modern Microbial Mats, Trends in Microbiology, 29, 204–213, 2021.

Whitton, B. A., Potts, M.: Introduction to the Cyanobacteria. In: *Ecology of Cyanobacteria II: Their Diversity in Space and Time* (ed. Whitton BA). Springer Netherlands, Dordrecht, pp. 1–13, 2012.

Zachos, J., Pagani, M., Sloan, L., Thomas, E., Billups, K.: Trends, Rhythms, and Aberrations in Global Climate 65 Ma to Present, Science, 292, 686–693, 2001.

Zeebe, R. E., Wolf-Gladrow, D. A.: CO_2 in seawater: Equilibrium, Kinetics, Isotopes, Amsterdam: Elsevier, 2001.

Zhang, C. L., Horita, J., Cole, D. R., Zhou, J., Lovley, D. R., Phelps, T. J.: Temperature-dependent oxygen and carbon isotope fractionations of biogenic siderite, Geochimica et Cosmochimica Acta, 65, 2257–2271, 2001.

https://doi.org/10.5194/egusphere-2026-3594
Preprint. Discussion started: 5 August 2026

Tables

Table 1. Major ion and carbonate chemistry for the different model scenarios

Model scenario	Ca (mmol/kg)	Mg (mmol/kg)	Na (mmol/kg)	K (mmol/kg)	Cl (mmol.kg)	SO_4 (mmol/kg)	DIC (mmol/kg)	pH	Alkalinity (mmol/kg)	$\delta 13C_{DIC}$ (‰)	$\delta 13C_{org}$ (‰)
Turks and Caicos Platform	10.2	52.6	464.5	10.1	540.5	27.9	2.1	*N/a*	2.4	0.7	-8.0
Great Salt Lake (South Arm)	4.5	156.0	1433.0	58.0	1659.0	78.0	3.7	*N/a*	4.6	-0.7	-8.0
Green Lake	9.8	2.5	1.2	0.1	0.6	9.8	2.5	*N/a*	2.4	-7.0	-14.3
Morrison Lake	9.8	2.5	1.2	0.1	0.6	9.8	*N/a*	7.6 (W)–8.7 (S)	3.5	-7.0	-14.3

Note that major ion chemistry values for Morrison Lake were adopted from Green Lake as these data have not been measured or published. For the Morrison Lake pH data, W refers to winter values and S refers to summer values. Morrison Lake pH data are available in Data Set S1.

https://doi.org/10.5194/egusphere-2026-3594
Preprint. Discussion started: 5 August 2026

1102 **Figures**

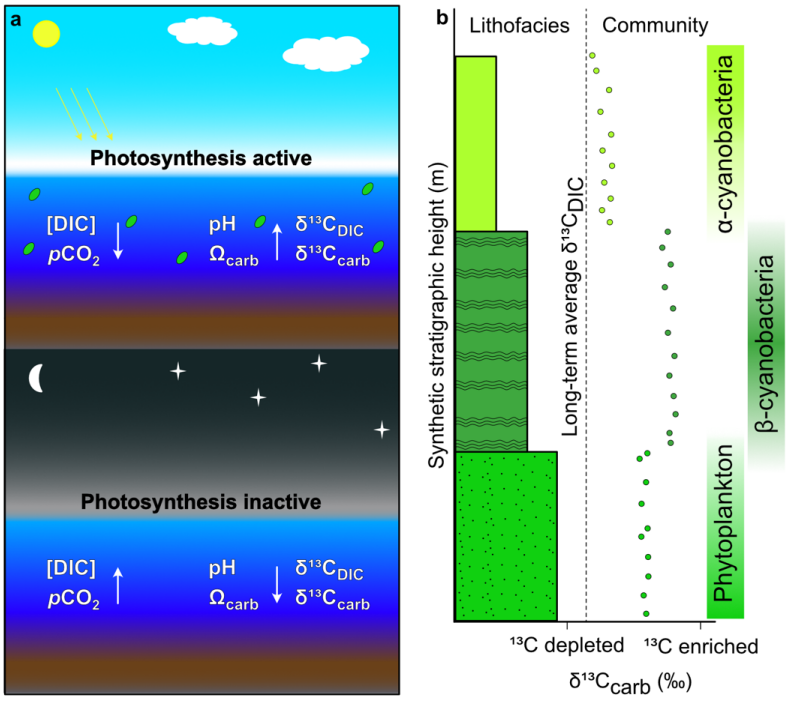

1103

1104 **Figure 1. Theoretical impact of the diurnal carbon engine on $\delta^{13}C_{carb}$ records. a**, a schematic
1105 depicting how the diurnal engine modulates carbonate geochemistry based on time of day. **b**, a
1106 theoretical stratigraphic column and corresponding precipitated $\delta^{13}C_{carb}$ record indicating how
1107 sedimentary lithofacies and the dominant phytoplankton community could drive fluctuations in
1108 $\delta^{13}C_{carb}$ values (modifying the local diurnal carbon engine) that do not reflect changes in long-term
1109 average $\delta^{13}C_{DIC}$ values but instead environmental/ecological change. Note that in **b** the shade of
1110 green indicates both sedimentary lithofacies and dominant phytoplankton community.

1111

https://doi.org/10.5194/egusphere-2026-3594
Preprint. Discussion started: 5 August 2026

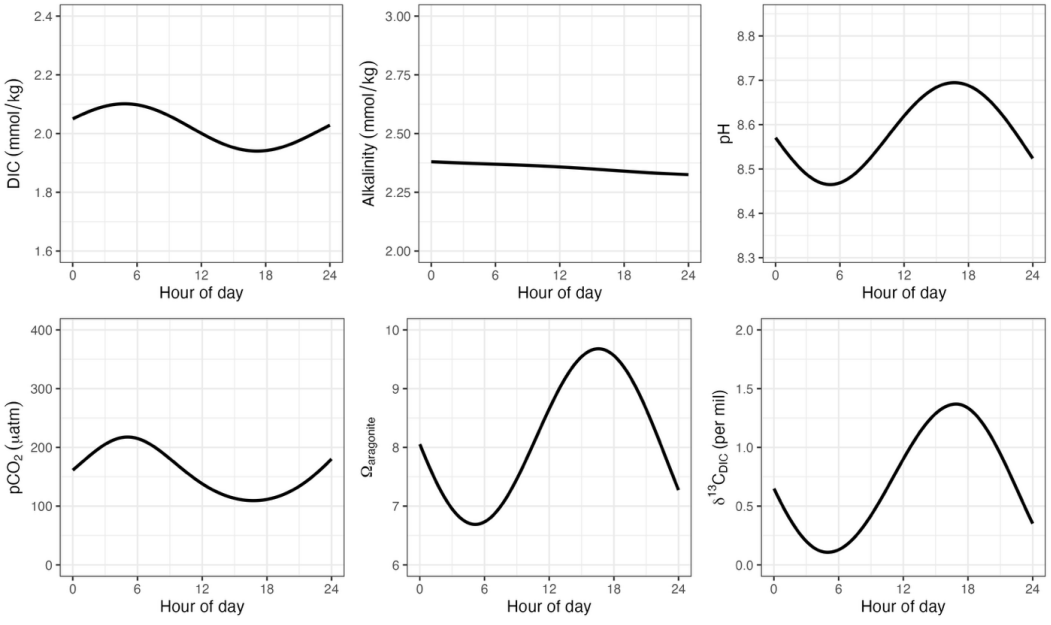

Figure 2. An open-source diurnal carbon engine model adapted to handle lake geochemistry. The diurnal carbon engine model (adapted from Trower et al. (2024)), with modifications to how geochemistry calculations are made to allow for lacustrine datasets. Diurnal variability in dissolved inorganic carbon concentration ([DIC]), alkalinity (Alk), pH, pCO_2, aragonite saturation state (Ω_{ar}), and the carbon isotopic value for DIC ($\delta^{13}C_{DIC}$) are plotted here for the Caicos Platform. These model outputs are identical to those detailed in Trower et al. (2024). Hour 0 represents 00:00 (midnight).

https://doi.org/10.5194/egusphere-2026-3594
Preprint. Discussion started: 5 August 2026

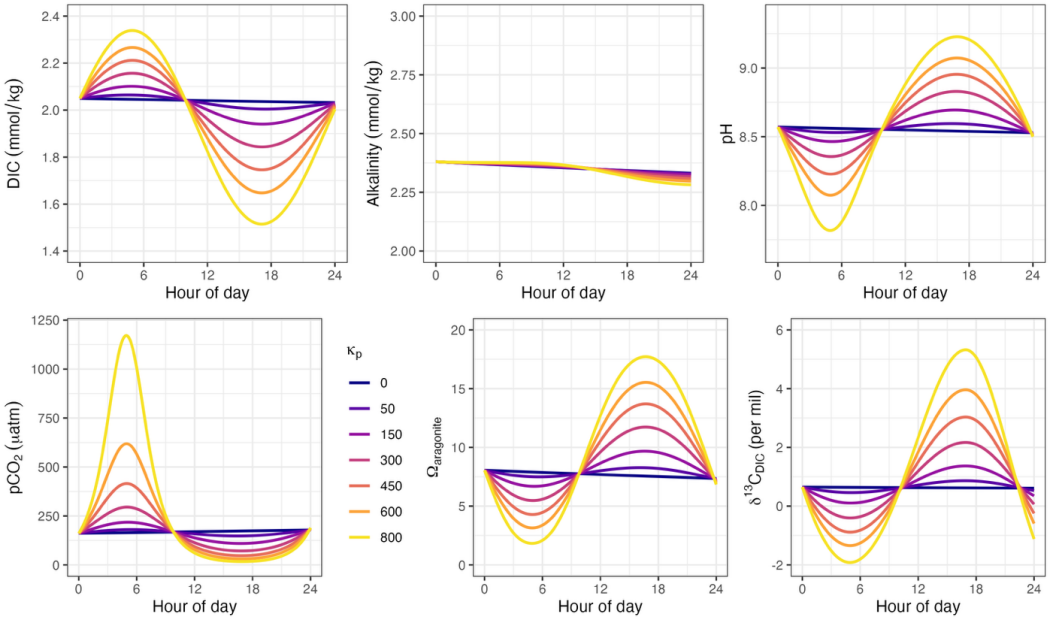

Figure 3. A sensitivity test exploring the impact of productivity on the diurnal carbon engine. K_p (reflecting photosynthetic forcing strength) is a key parameter in shaping the photosynthetic carbon flux in the diurnal carbon engine model yet has only been constrained in marine settings (see Trower et al., 2024). We vary the value of K_p from 0–800 (see pCO_2 panel for color-coded legend) for the Caicos Platform and find that greater values of K_p (and therefore a stronger diurnal carbon engine) lead to a greater response in carbonate geochemistry parameters including dissolved inorganic carbon concentration ([DIC]), pH, pCO_2, aragonite saturation state (Ω_{ar}), and the carbon isotopic value for DIC ($\delta^{13}C_{DIC}$), with the exception of alkalinity (alk). Hour 0 represents 00:00 (midnight).

https://doi.org/10.5194/egusphere-2026-3594
Preprint. Discussion started: 5 August 2026

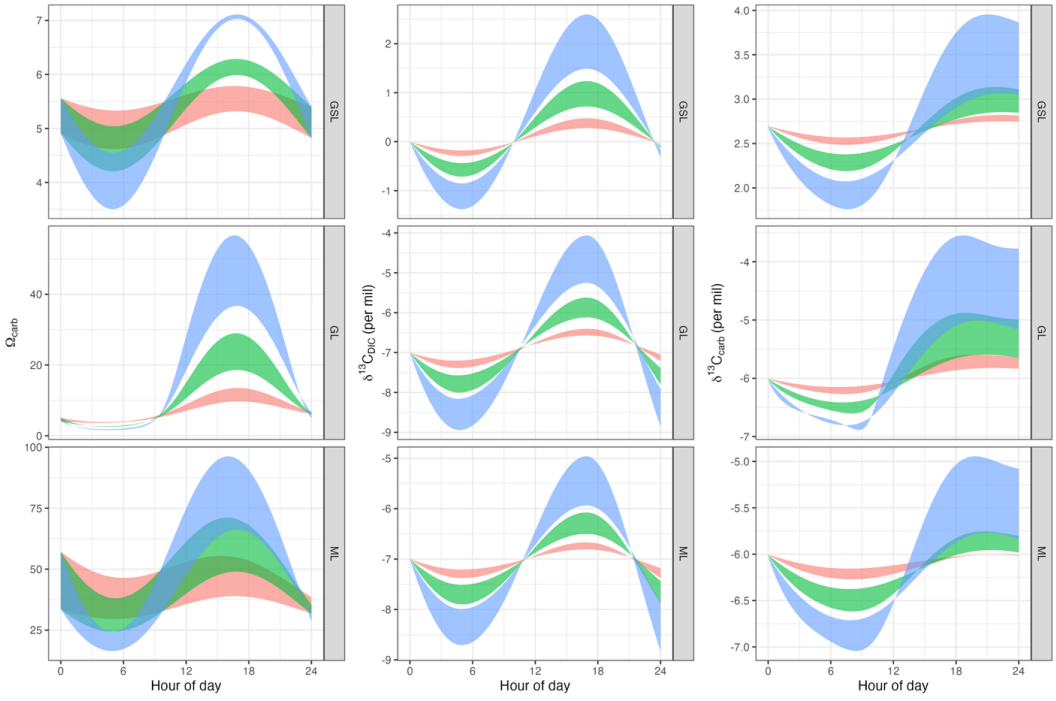

Figure 4. Lake chemistry, seasonality, and phytoplankton community affect the strength of the diurnal carbon engine. The impact of the diurnal carbon engine on carbonate saturation state (Ω_{carb}; left column), the carbon isotope value of dissolved inorganic carbon ($\delta^{13}C_{DIC}$; center column), and the cumulative carbon isotope value of carbonate ($\delta^{13}C_{carb}$; right column) according to lake chemistry, seasonality, and phytoplankton community is shown in nine panels. Panels are positioned according to lake, with those in the top row Great Salt Lake (South Arm; model scenario 2), those in the middle row representing Green Lake (model scenario 3), and those in the bottom row representing Morrison Lake (model scenario 4). Each panel depicts three model envelopes: $K_p = 150$ in red, $K_p = 375$ in green, and $K_p = 750$ in blue. The upper bound of each model envelope corresponds to summer conditions, while the lower bound corresponds to winter conditions with reduced temperature (5°C versus 25°C) and photosynthetic forcing (60% of summer forcing). In every scenario, $\delta^{13}C_{carb}$ values (right column) do not return to their initial values, indicating the change in the isotopic value of the accumulated carbonate over the course of the day. Hour 0 represents 00:00 (midnight).

https://doi.org/10.5194/egusphere-2026-3594
Preprint. Discussion started: 5 August 2026

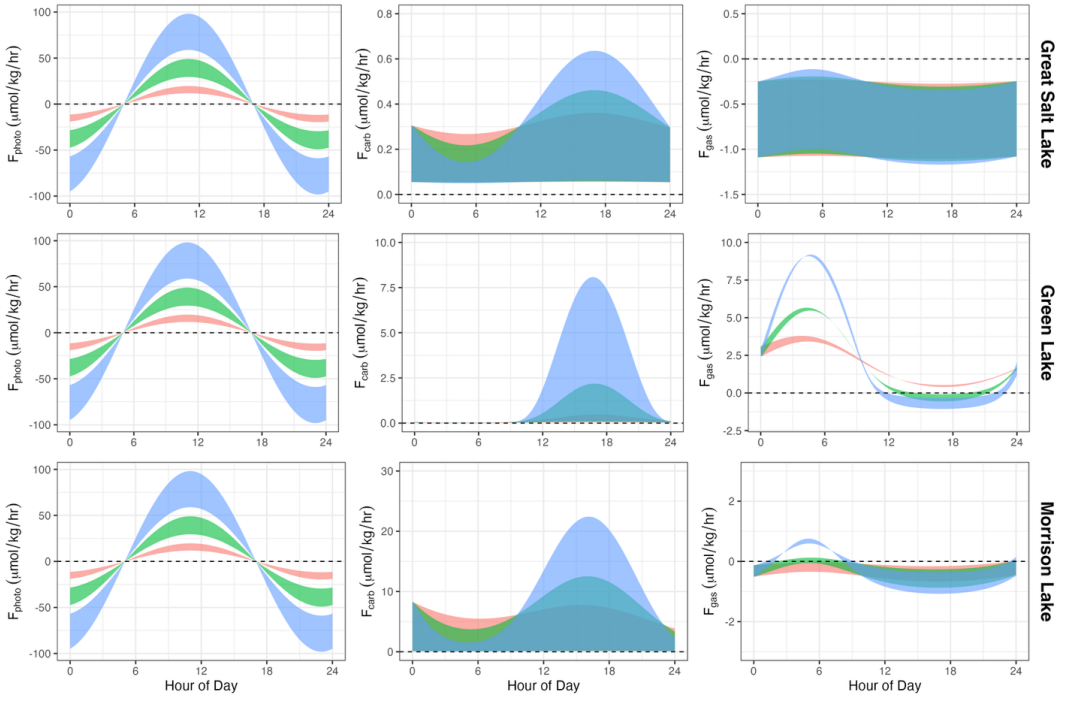

Figure 5. Resulting carbon fluxes when modeling the impact of lake chemistry, seasonality, and phytoplankton community on the diurnal carbon engine. Modeled photosynthetic flux (F_{photo}; left column), carbonate precipitation flux (F_{carb}; center column), and gas exchange flux (F_{gas}; right column) according to lake chemistry, seasonality, and phytoplankton community is shown in nine panels. Panels are positioned according to lake chemistry as in Figure 4, with those in the top row representing Great Salt Lake (South Arm; model scenario 2), those in the middle row representing Green Lake (model scenario 3), and those in the bottom row representing Morrison Lake (model scenario 4). As in Figure 4, each panel depicts three model envelopes: K_p = 150 in red, K_p = 375 in green, and K_p = 750 in blue. The upper bound of each model envelope corresponds to summer conditions, while the lower bound corresponds to winter conditions with reduced temperature (5°C versus 25°C) and photosynthetic forcing (60% of summer forcing). Hour 0 represents 00:00 (midnight).

https://doi.org/10.5194/egusphere-2026-3594
Preprint. Discussion started: 5 August 2026

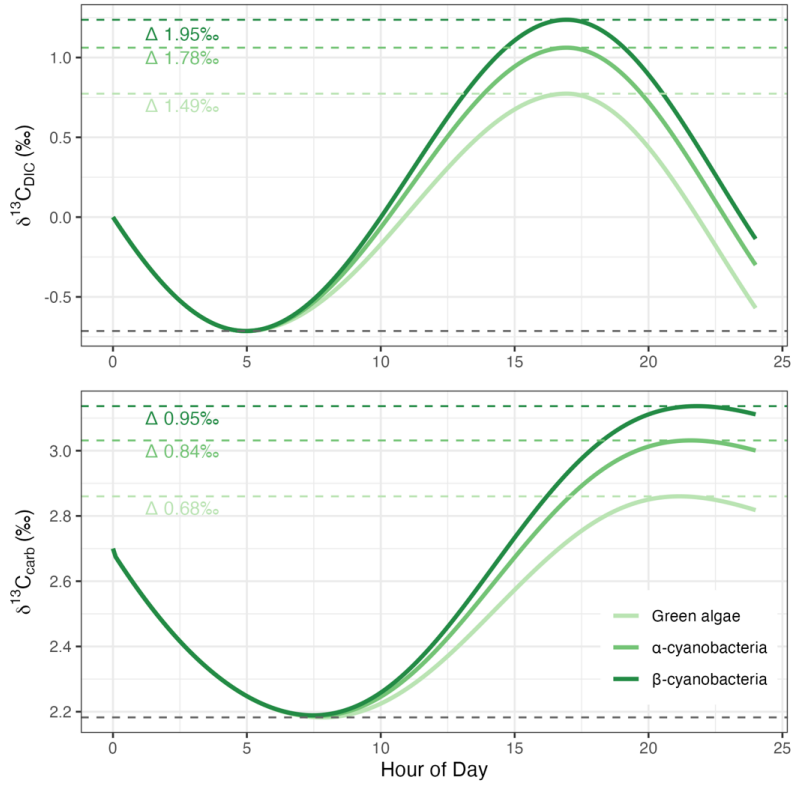

Figure 6. Impact of dominant phytoplankton community on the isotopic response to the diurnal carbon engine. Using Great Salt Lake geochemistry, we varied the ε_p according to phytoplankton community to simulate the impact of different communities (β-cyanobacteria, α-cyanobacteria, and green algae; see legend) on the diurnal carbon engine. Due to the associated ε_p, α-cyanobacteria resulted in the highest $\delta^{13}C_{DIC}$ (above) and $\delta^{13}C_{carb}$ values (below) and the strongest diurnal carbon engine effect (with green algae and β-cyanobacteria resulting in a progressively smaller impact, respectively). The impact of the phytoplankton community on $\delta^{13}C_{DIC}$ values is larger than on $\delta^{13}C_{carb}$ values. Hour 0 represents 00:00 (midnight).

https://doi.org/10.5194/egusphere-2026-3594
Preprint. Discussion started: 5 August 2026

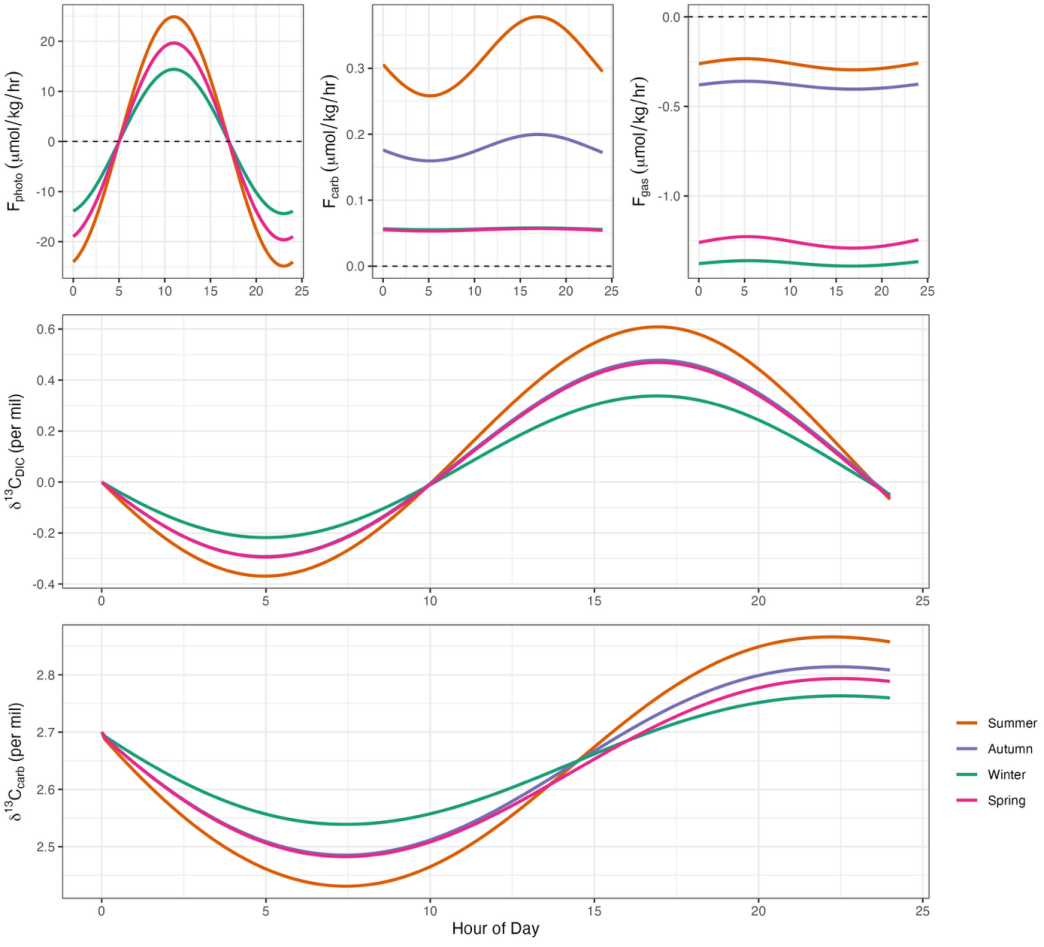

Figure 7. Isolating the impact of seasonality on the diurnal carbon engine in Great Salt Lake. Because we have the most extensive data for Great Salt Lake, we model Great Salt Lake during summer (orange lines), autumn (purple lines), winter (green lines), and spring (magenta lines), modifying temperature (T = 25°C, 18°C, -3°C, and 5°C, respectively), average wind speed (u = 4.1 m/s, 3.8 m/s, 3.3 m/s, and 4.3 m/s, respectively), and estimated productivity (κ_p = 190, 150, 110, and 150, respectively). Resulting carbon fluxes (photosynthetic flux, F_{photo}; carbonate precipitation flux, F_{carb}; and gas exchange flux, F_{gas}) for these seasonal model simulations are shown in the top row. Note that in the F_{photo} panel the spring (green) and autumn (red) simulations result in identical F_{photo}, with the autumn simulation obscuring the spring simulation. In the upper center panel, the estimated F_{carb} during spring (green) and winter (blue) overlap, making the individual lines difficult to see. The center panel shows the modeled carbon isotope value of dissolved inorganic carbon ($\delta^{13}C_{DIC}$) for each seasonal simulation. As was the case in the F_{photo} panel, the autumn simulation (red) obscures the spring simulation (green) in this panel. The bottom panel shows the modeled cumulative carbon isotope value of carbonate ($\delta^{13}C_{carb}$) for each seasonal simulation. Hour 0 represents 00:00 (midnight).

https://doi.org/10.5194/egusphere-2026-3594
Preprint. Discussion started: 5 August 2026

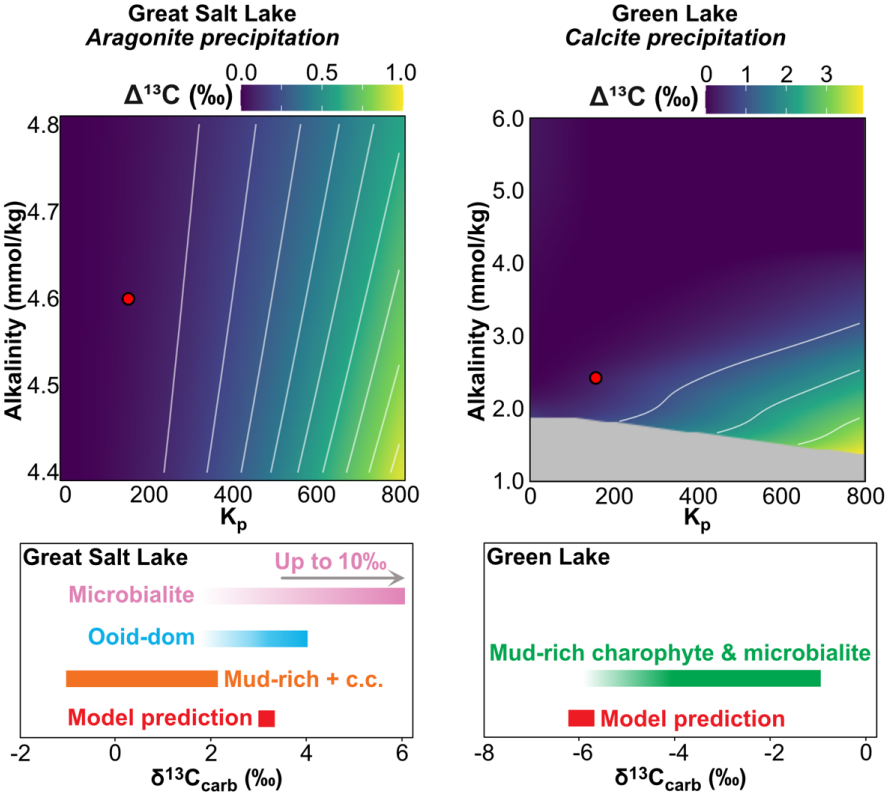

Figure 8. Broader implications of the diurnal carbon engine on lacustrine $\delta^{13}C_{carb}$ records. Contour plots show the predicted isotopic offset ($\Delta^{13}C$) between carbonate precipitated under an active diurnal carbon engine and carbonate precipitated from dissolved inorganic carbon (DIC) in equilibrium with long-term average $\delta^{13}C_{DIC}$, for Great Salt Lake (aragonite; left) and Green Lake (calcite; right), as a function of productivity (κp) and alkalinity. $\Delta^{13}C$ is defined as the difference between precipitation-weighted mean $\delta^{13}C_{carb}$ and the daily average instantaneous $\delta^{13}C_{carb}$ value (expected daily variability). Warmer colors indicate larger positive offsets. Red dots denote representative modern lake conditions used to estimate expected daily variability in $\delta^{13}C_{carb}$. In regions of parameter space where carbonate precipitation is limited or absent, $\Delta^{13}C$ approaches zero, indicating that diurnal variability does not necessarily translate to isotopic bias. Grey regions in the Green Lake panel indicate parameter combinations where calcite saturation state remains below 1 throughout the diurnal cycle, precluding carbonate precipitation and yielding no $\Delta^{13}C$ signal. Bottom panels compare modeled $\delta^{13}C_{carb}$ values with previously reported measurements from different sedimentary components in Great Salt Lake and Green Lake.

https://doi.org/10.5194/egusphere-2026-3594
Preprint. Discussion started: 5 August 2026

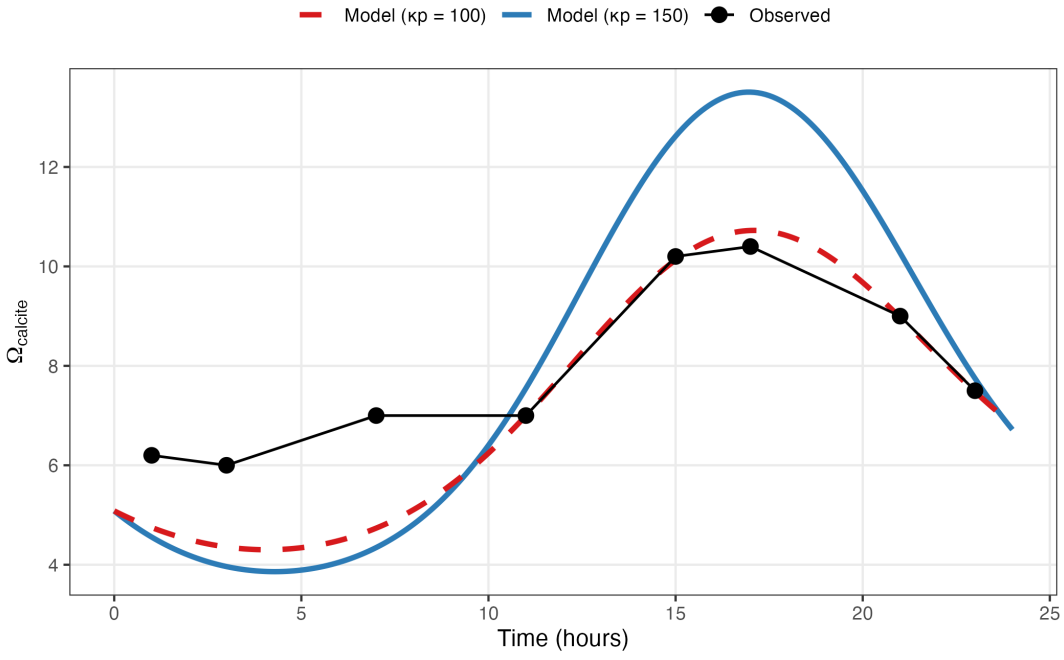

Figure 9. Comparison of modeled and observed diurnal variability in calcite saturation state (Ω). Observations from Green Lake (0.25 m depth; July 28–29, 1978; Effler et al., 1981, Fig. 3a) are shown as black points, and model results are shown as continuous lines. Model simulations are shown for two productivity scenarios (κp = 100, dashed red line; κp = 150, solid blue line), illustrating the sensitivity of diurnal variability to photosynthetic forcing. Observed data were temporally aligned to the modeled peak to account for differences in time reference frames. The model reproduces the timing and overall structure of the observed diurnal cycle, while the magnitude of variability is controlled by productivity, demonstrating that the model captures first-order dynamics of biologically mediated carbonate chemistry in lacustrine systems.